nature communications

Article

https://doi.org/10.1038/s41467-026-73896-2

The vagus nerve promotes memory in rats via nutrient-induced septo-hippocampal acetylcholine signaling

Received: 14 July 2025

Accepted: 22 May 2026

Published online: 04 June 2026

Check for updates

Logan Tierno Lauer[1], Anna M. R. Hayes[1], Andrea N. Suarez[1,2], Alexander Bashaw[1], Molly E. Klug[1], Alicia E. Kao[1], Robert Cheng[1], Jessica J. Rea[1,2], Keshav S. Subramanian[1,2], Anna Nourbash[1], Kristen N. Donohue[1], Lindsey A. Schier[1,2], Kevin Myers[3], Léa Décarie-Spain[1,4,5] & Scott E. Kanoski[1,2]

The vagus nerve relays critical metabolic information between the gastrointestinal tract and the brain. Recent findings highlight a role for vagus nerve-mediated gut-brain signaling in regulating higher-order cognitive processes, although the underlying mechanisms remain poorly understood. Here we demonstrate in male rats that nutrient consumption promotes hippocampal-dependent memory function via vagus nerve-mediated acetylcholine (ACh) release in the dorsal hippocampus (HPCd) from medial septum (MS) neurons. In vivo fiber photometry analyses reveal that HPCd ACh release is engaged during nutrient consumption. This response was abolished in animals that received MS cholinergic neuron ablation, subdiaphragmatic vagotomy (SDV), or early-life Western Diet (WD) maintenance. MS cholinergic neuron ablation, SDV, and WD impaired memory for meal location, suggesting that this signaling pathway functions to promote memories for eating events. Collectively, results identify a neurobiological mechanism whereby nutrient consumption enhances memory function and suggest that disruption of this vagal-brain signaling system mediates WD-associated memory impairments.

Communication between the gastrointestinal (GI) tract and the brain is critical in maintaining food intake control and overall energy regulation[1–4]. Emerging work also identifies a role for the gut-brain axis in higher-order cognitive functions[5,6]. A key conduit of communication between the gut and the brain is the vagus nerve, whose afferent/sensory neurons (vagal afferent neurons, VAN) transmit a wide array of metabolic information from the GI tract to the central nervous system[7]. Recent evidence indicates that VAN influences on brain processes extend beyond traditional brainstem targets to include transsynaptic communication to higher-order structures involved in cognition, including the hippocampus (HPC)[8–12], a critical mediator of episodic and spatial navigation-based memory[13–15].

The medial septum (MS) is an anatomical relay of neural communication between the caudal brainstem, where GI VAN synapses, and the dorsal subregion of the hippocampus (HPCd)[10]. The MS contains a population of acetylcholine (ACh)-producing neurons, and septo-hippocampal cholinergic signaling promotes hippocampal plasticity and memory encoding[16–18]. However, the upstream mechanisms that regulate septo-hippocampal memory systems are poorly understood. Here, we posit that this memory-promoting

[1]Human and Evolutionary Biology Section, Department of Biological Sciences, University of Southern California, Los Angeles, CA, USA. [2]Neuroscience Graduate Program, University of Southern California, Los Angeles, CA, USA. [3]Department of Psychology, O'Leary Center, Bucknell University, Lewisburg, PA, USA. [4]Centre de recherche du CHUM, Université de Montréal, Montreal, QC, Canada. [5]Department of Nutrition, Université de Montréal, Montreal, QC, Canada. e-mail: lea.decarie-spain@umontreal.ca; kanoski@usc.edu

circuitry is guided by visceral sensory pathways, including GI meal-associated signals transmitted to the brain via the VAN.

Consumption of a high-fat and sugar-enriched "Western diet" (WD) impairs HPC-dependent memory and associated neural processes, particularly when consumed during early life periods of development[19–22]. Recent findings reveal that early life WD exposure compromises HPC function through dysregulated HPC cholinergic signaling[23]. In parallel, WD consumption and obesity are linked with blunted VAN signaling, as animals exposed to WD demonstrate reduced brainstem responsiveness to satiation signals that are transmitted through VAN[24–28]. Furthermore, vagus nerve ablation through sub-diaphragmic vagotomy (SDV) or through sensory-specific cholecystokinin-conjugated saporin-mediated VAN ablation disrupts HPC-dependent memory function in rats, coupled with reductions in HPC markers of synaptic plasticity and neurogenesis (brain-derived neurotrophic factor and doublecortin, respectively)[10]. Consistent with these findings, either gastric distension or intestinal nutrient infusion robustly enhances cerebral blood flow to the HPC[29,30]. Collectively, these findings highlight a putative functional connection between GI VAN and septo-hippocampal ACh signaling, and raise the possibility that WD-associated cognitive deficits may stem, in part, from a breakdown in this gut-VAN-HPC connection.

In the present study we elucidate how GI-originating VAN signaling modulates HPC function. Results identify a role for nutritive signals in driving HPC-dependent memory. Eating behavior dynamically increases HPC ACh release, and these levels remain elevated after a meal. These effects are eliminated by either VAN ablation or MS ACh neuron deletion, and are also negatively impacted by an early-life junk food diet. These data collectively define mechanisms that reveal how and where gut-vagus-HPC communication promotes memory, and provide mechanistic insights into how interoceptive dysfunction may contribute to cognitive decline.

Results

The gut peptide CCK promotes hippocampal activity via septal cholinergic neurons

Cholecystokinin (CCK) is an intestinally-derived hormone that promotes satiation and meal termination predominantly through paracrine action on the vagus nerve in response to the presence of nutrients in the small intestines[31]. The medial septum (MS) is an anatomical relay connecting the caudal brainstem (where gut-derived VAN converge) to the HPC[10], and thus the MS may communicate gut vagal signaling to the HPC. To explore this hypothesis, rats were injected with either a 192IgG saporin immunotoxin in the MS (to ablate MS cholinergic neurons) or a control saporin (Fig. 1a). Following surgical recovery, the animals received peripheral administration (intraperitoneal; IP) of either vehicle (saline) or CCK (3 µg/kg; a dose that requires the vagus nerve for food intake reduction[1]), and immunofluorescence analyses were conducted to quantify c-Fos protein expression in the dentate gyrus (DG) and CA3 subregions of the dorsal HPC (HPCd). Results revealed that, relative to vehicle treatment, IP CCK elevated c-Fos expression in the DG granular layer and in the dorsal CA3 (CA3d) pyramidal layer in animals who received MS control saporin treatment. However, MS 192IgG saporin injections eliminated IP CCK-induced HPCd c-Fos induction, with expression comparable to vehicle treatments (Fig. 1b, c and Supplementary Fig. 1a, b). To further corroborate that MS ACh transmission is engaged in the HPC by peripheral CCK, rats were injected with an pAAV.hSynap.iAChSnFR and an optic fiber cannula in the HPCd (DG) to detect fluctuations in ACh release in vivo in awake and freely behaving animals that received either 192IgG saporin or control saporin in the MS (Fig. 1d, e). Post surgical recovery, fiber photometry was used to measure HPCd ACh release in response to IP vehicle or CCK administration following an overnight fast (Fig. 1f). Results revealed a sustained (~10–40 min after injections) elevation in HPCd ACh release after IP CCK administration relative to vehicle administration in animals with MS control saporin treatment; an effect that was eliminated by ablation of cholinergic neurons in the MS (Fig. 1g–i). To examine whether this effect is specific to vagally-mediated peptide signals, we next evaluated HPCd ACh release in response to IP vehicle vs amylin, a pancreatic hormone with food intake-reducing effects that do not require the vagus nerve[32]. In contrast to CCK, amylin did not elicit any responses in HPCd ACh signaling relative to vehicle treatments (Supplementary Fig. 1d). Together, these data reveal that CCK, a gut-derived peptide signal that acts through the vagus nerve, promotes HPCd ACh activity via MS cholinergic neurons.

Meal consumption enhances hippocampus acetylcholine signaling

To evaluate HPCd ACh responses during physiological engagement of GI VAN, we recorded ACh release during meal consumption of standard chow after an overnight fast. Timestamps were taken to analyze cholinergic activity during active eating periods (composed of eating bouts; i.e., the animal is actively eating) vs. inter bout-periods (i.e., the periods between active eating bouts, during which animals are typically rearing or exploring) (Fig. 2a). Results revealed that, on average, HPCd ACh release z-score is lower over a 15-s period after an active eating bout starts compared to 15 s before the same eating bout ends (Fig. 2e). In contrast to this, we observed that HPCd ACh release stayed elevated over a 15-s period after an eating bout was terminated, and was reduced over the 15 s period before the subsequent eating bout was initiated (Fig. 2f). These findings suggested that HPCd ACh release dynamically increases during active eating bouts, with levels increasing from the start to the end of an eating bout. The opposite pattern was observed during inter-bout periods, where ACh release dynamically reduced from the beginning to the end of the break in eating, thus yielding a significant difference in the delta for ACh release during active eating vs. inter-bout periods (representative trace from a single animal in Fig. 2b; zoomed-in trace shown in Supplementary Fig. 2a, b; compiled group data in Fig. 2c, d).

Given the variability in the duration of active eating bouts and interbout intervals, we sought to better elucidate whether the temporal features of HPCd ACh dynamics during food consumption could be explained by bout and interbout duration. In doing so, eating bouts and interbout intervals were divided into meal phase tertiles (early, middle, and late) irrespective of their duration. Across each tertile, the slope of HPCd ACh release (*z*-score/minute) was computed, and a simple linear regression model was fitted to assess the relationship between the slope of HPCd ACh release across different phases of eating bouts and interbouts (tertiles) and their durations. Results revealed a significant negative relationship between eating bout duration and the slope of HPCd ACh release during early and middle phases of eating bouts (Supplementary Fig. 2k, l). Meanwhile, there was a significant positive relationship between eating bout durations and the slope of HPCd ACh release at late phases of eating bouts (Supplementary Fig. 2m). In contrast to this, we found no relationship between interbout durations and the slope of HPCd ACh release (Supplementary Fig. 2n–p).

To further elucidate the temporal features of HPCd ACh The average ACh release during the entirety of active eating bouts, however, did not differ from interbout intervals (Supplementary Fig. 2c). To better understand the dynamic fluctuations during these behavioral epochs, we focused on behavioral transition switch points and found that the slope of ACh release shifted upwards within a few (~10) seconds after an eating bout started (Fig. 2e) and shifted downwards immediately after a bout terminated (Fig. 2f). To determine whether the dynamic elevation in HPC ACh during eating bouts vary as a function of meal period, ΔHPCd ACh responses during eating bouts were compared across tertiles representing early, middle, and late meal periods. Results revealed that the increases in

https://doi.org/10.1038/s41467-026-73896-2

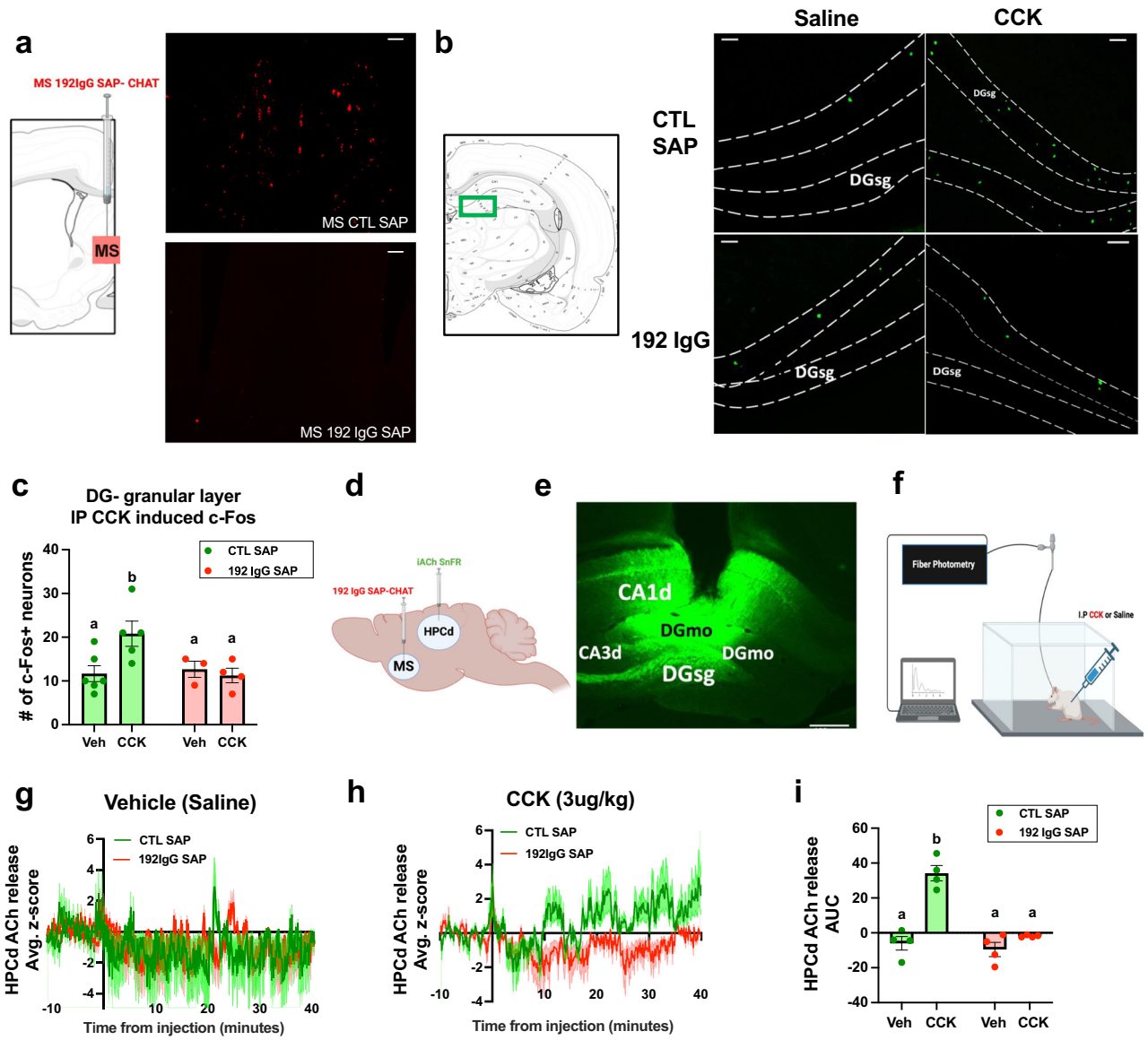

Fig. 1 | Peripheral CCK engages hippocampal activity via septal cholinergic neurons. a Schematic and representative medial septum (MS) images of immunoreactive CHAT+ neurons in an animal with control saporin (top) and 192IgG saporin toxin (bottom). Scale bar = 30 microns. **b** Schematic and representative images of dorsal dentate gyrus granular layer immunoreactive c-Fos+ neurons in control saporin and 192IgG saporin treated animals given IP CCK (3 µg/kg) or vehicle (saline). Scale bar = 30 microns. **c** Dorsal dentate gyrus granular layer c-Fos+ neurons quantification. ($n = 6$ Vehicle-CTL SAP; $n = 4$ CCK-CTL SAP; $n = 3$ Vehicle-192IgG sap; $n = 4$ CCK-192IgG SAP). Data were analyzed using two-way ANOVA with multiple comparisons. Treatment data with the same letter above are not significantly different. IP Treatment x saporin interaction $P = 0.0066$, CTL SAP Vehicle vs CCK $^{**}P = 0.0026$; CCK treatment CTL SAP vs. 192IgG SAP $^{**}P = 0.0045$. **d** Schematic of surgical approach for 192IgG SAP in MS and iAChSnFR in HPCd (created in BioRender. Kanoski, S. (2026) https://BioRender.com/8dtm80o). **e** Representative HPCd image of GFP immunoreactive neurons containing iAChSnFR, scale bar = 100 microns. **f** Schematic of fiber photometry recordings during IP CCK and vehicle treatments. **g** Time-locked averaged HPCd ACh release to IP vehicle administration ($n = 4$ Vehicle-CTL SAP; $n = 4$ Vehicle-192IgG SAP). **h** Time-locked averaged HPCd ACh release to IP CCK (3 µg/kg) administration ($n = 4$ CCK-CTL SAP; $n = 4$ CCK-192IgG SAP). **i** HPCd ACh release AUC quantification in response to IP vehicle and CCK administration ($n = 4$ CCK-CTL SAP; $n = 4$ CCK-192IgG SAP). Treatment data with the same letter above are not significantly different. Data were analyzed using two-way ANOVA with multiple comparisons (see "Statistical methods"); IP Treatment x saporin interaction $^{**}P = 0.0016$; CTL SAP-Veh vs. CCK $^{***}P = 0.0006$; CCK treatment CTL SAP vs. 192IgG SAP $^{***}P = 0.0008$. Data are shown as mean ± SEM; $^{****}P < 0.0001$, $^{**}P < 0.01$. Source data are provided as a Source Data file.

ΔHPCd ACh during eating bouts were significantly larger in magnitude during later consumption bouts (bouts occurring in the third tertile of a meal) compared to earlier ones (bouts occurring within the first tertile of a meal), whereas ΔHPCd ACh during inter-bout periods did not vary as a function of meal period (Supplementary Fig. 2d, e). Collectively, these findings reveal opposing dynamics shifts in the slope of ACh release shortly after behavior transitions between active eating and inter-bout periods, indicating that this neurochemical response is tightly coupled to behavior.

To determine whether HPCd cholinergic tone varied from the hungry (pre-meal) to the satiation (post-meal) state, we compared ACh release for a 5-min period before food access to a 5-min period after meal termination. Results revealed that HPCd ACh release was significantly elevated 5-min after meal termination compared to 5-min pre food consumption period (Fig. 2g, h).

Additionally, these food consumption-induced HPCd ACh responses were absent in animals that received 192IgG saporin in the MS relative to controls (Fig. 2i, j), despite there being no differences in

https://doi.org/10.1038/s41467-026-73896-2

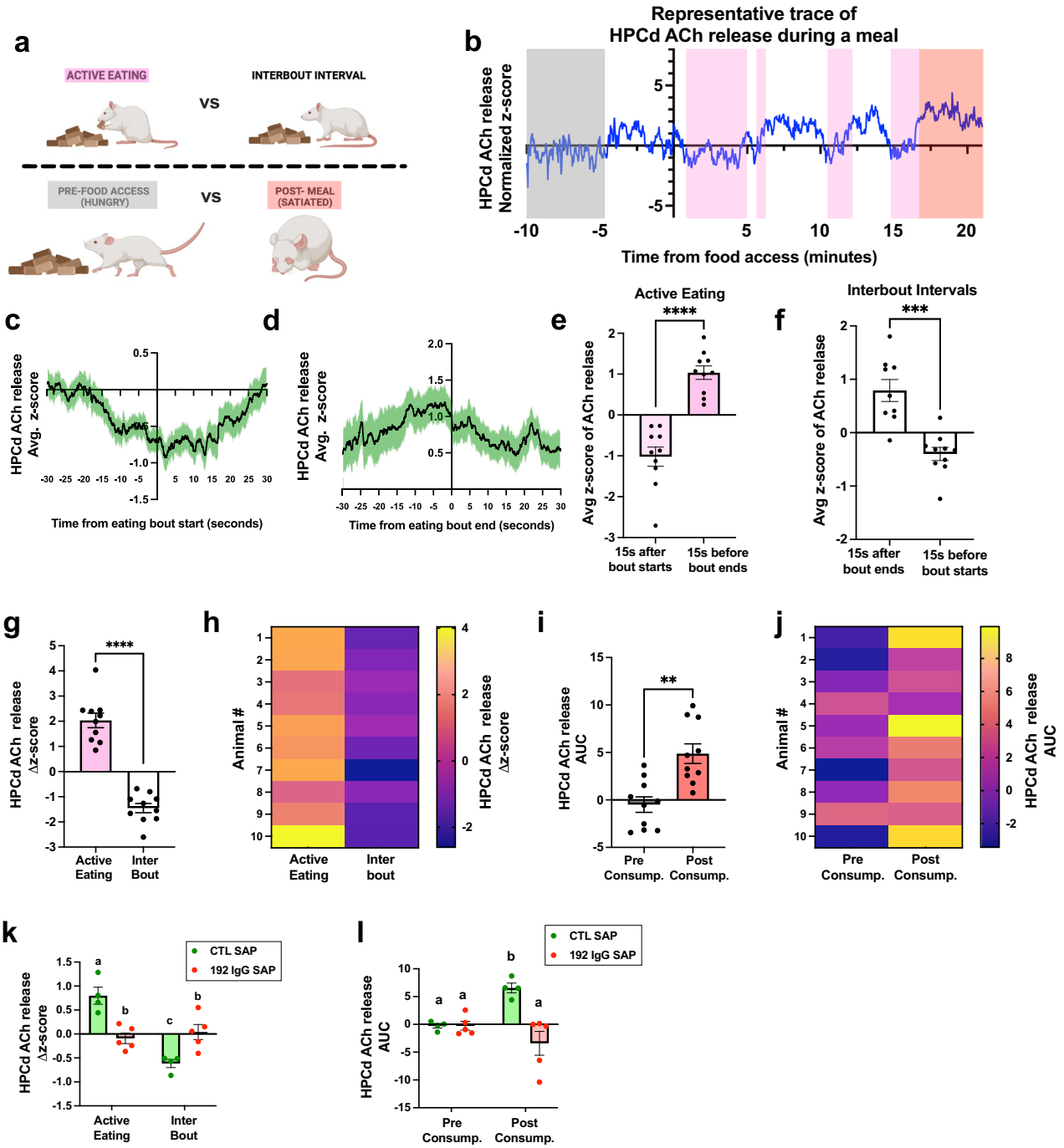

the amount of food consumed (Supplementary Fig. 2f). Meal period assessments in animals with control saporin reveal nonsignificantly larger ACh responses during later consumption bouts vs. earlier (Supplementary Fig. 2g, h). Collectively, these findings demonstrate that HPCd ACh release is highly responsive to naturalistic eating behavior, as demonstrated by its dynamic and sustained responses during active consumption periods and during satiated states. These results also further highlight the role of MS ACh neurons in HPCd responses to physiological engagement of the GI tract.

Consumption-driven elevations in hippocampal acetylcholine responses require nutrients

HPCd ACh responses during meal consumption may be driven by the caloric consequences of the food, by specific macronutrients, by oral sensory stimuli (e.g., taste), and/or by the locomotive action of eating. To dissociate between these possibilities, we evaluated dynamic HPCd ACh responses during consumption of isolated macronutrients vs. no- and low-calorie sweetened solutions (Fig. 3a). Results revealed that active consumption of an 11% sucrose solution induced the dynamic elevations in HPCd ACh release as previously observed with standard chow (Fig. 3b). The sustained elevation in cholinergic tone after voluntary termination of the 11% sucrose solution relative to the pre-consumption hunger state was also observed (Fig. 3b). Meal period analyses also revealed that ΔHPCd ACh release during later consumption bouts of 11% sucrose were significantly higher in magnitude than earlier ones, while there was no difference between the magnitude of ΔHPCd ACh release during early inter bout intervals vs. late ones (Supplementary Fig. 3a, b). Next, we assessed whether a calorically matched solution of 4.5% corn oil (pure lipid) would recapitulate these responses. Like carbohydrate consumption, lipid ingestion also elicited HPCd ACh

Fig. 2 | Meal consumption elevates septo-hippocampal cholinergic signaling. **a** Schematic of events timestamped during fiber photometry recordings while animals consume a meal. **b** Representative trace of HPCd ACh release during consumption of standard chow, time locked to the moment of access to food. Pre-consumption period (fasted state) is marked in the gray box, active eating periods [pink boxes; quantified as the Δ in activity between start and end of eating bout], inter bout intervals [white boxes; quantified as the Δ in activity between the end of an eating bout and the beginning of the subsequent eating bout], and post-consumption period (satiated state) marked in the red box are represented. **c**, **d** Time-locked averaged HPCd ACh release activity around the start of eating bouts (**c**) and the end of eating bouts (**d**). **e** Fiber photometry recording of HPCd ACh release quantification during meal consumption (data analyzed using Student's two-tailed paired *t*-test, $n = 10$ rats) with **e** displaying the average z-score of ACh release 15-s after the active eating bout starts and 15-s before the eating bout ends. (data analyzed using a Student's two-tailed paired *t*-test, $n = 10$ rats; 15 s after bout starts vs. 15 s before bout ends $^{****}P = 0.000023$). **f** Average z-score of ACh release 15-s after eating bout ends, and 15-s before subsequent eating bout starts (15 s after bout end vs. 15 s before bout starts $^{***}P = 0.0001$). **g** Change in HPCd ACh release *z*-score during active eating periods [pink boxes] and inter bout intervals [white boxes], $^{****}P = 0.000017$ ($n = 10$ rats). Analyzed via paired, two-tailed, student's *t*-test. **h**. Individual animal values of change in HPCd ACh release during active eating and interbout intervals. **i**. Area under curve (AUC) HPCd ACh release during 5-min pre-food consumption (fasted state; gray box) and 5-min post-food consumption (satiated state; red box), ($n = 10$ rats) $^{**}P = 0.0054$, (Analyzed via paired, two-tailed, student's *t*-test), and **j** individual animal values of HPCd ACh release AUC during pre- and post-consumption periods. **k**, **l** Fiber photometry recordings of HPCd ACh release during food consumption in animals with either control saporin (CTL SAP; green), or 192IgG SAP (red) in the MS. All treatment data containing the same letter above are not significantly different, with **k** depicting the change in ACh release during active eating bouts and inter bout intervals for both experimental groups. Saporin treatment x eating period interaction $^{**}P = 0.0027$. CTL SAP, active eating vs. inter bout $^{***}P = 0.0007$; Active eating, CTL SAP vs. 192IgG SAP $^{**}P = 0.0082$; Inter bout, CTL SAP vs. 192IgG SAP $^{*}P = 0.0325$. **l** HPCd ACh release AUC quantification during pre-consumption and post-consumption periods. Saporin treatment x energy state interaction $P = 0.053$. CTL SAP, pre-consumption vs. post-consumption. Data were analyzed using two-way ANOVA with multiple comparisons (see "Statistical methods"), ($n = 4$, CTL SAP; $n = 5$, 192IgG SAP) $^{*}P = 0.015$; Post-consumption, CTL SAP vs. 192IgG SAP $^{**}P = 0.0061$. Data are shown as mean ± SEM; $^{****}P < 0.0001$, $^{**}P < 0.01$. Source data are provided as a Source Data file.

responses during its active consumption periods, as well as a sustained elevation in ACh release after meal termination (Fig. 3c). ΔHPCd ACh responses were larger in magnitude during later consumption bouts than earlier, but these analyses did not reach significance (Supplementary Fig. 3c, d). To interrogate whether these consumption-induced cholinergic responses were due to caloric content, we conducted the same experiment with 0.2% saccharin, which is an artificial sweetener that will engage sweet taste receptors but is devoid of calories. Results revealed no differences in ΔHPCd ACh release during active consumption of 0.2% saccharin vs. inter bout intervals, nor was there differential ACh release in the post- vs. pre-consumption period (Fig. 3d). However, the animals consumed significantly less of the 0.2% saccharin solution compared to 11% sucrose or the 4.5% corn oil solutions (Fig. 3f), and thus the different ACh response profiles may be based on volume of solution consumed and not caloric content. To control for ingestion volume while keeping caloric content very low, we repeated the experiment with a solution combining 0.2% saccharin with the addition of 2% sucrose, which resulted in consumption levels (volumes of solution) that were significantly higher than that of 11% sucrose and 4.5% corn oil (Fig. 3f). Fiber photometry readings revealed no differences in ΔHPCd ACh release during active consumption of the 0.2% saccharin + 2% sucrose solution vs. inter bout intervals, and there was no difference in ACh tone between fasted and post-consumption states (Fig. 3e). Further, there was no difference in the ΔHPCd ACh release during active consumption bouts and inter bout intervals across meal period stages for either the 0.2% saccharin or the 0.2% saccharin + 2% sucrose solutions (Supplementary Fig. 3e–h). Together, these findings reveal that consumption-induced HPCd ACh engagement requires sufficient nutritive feedback.

Meal- and CCK-induced elevations in hippocampal acetylcholine responses require the vagus nerve

Given that signals arising from gut macronutrient detection are transmitted via a variety of pathways[33–35], we next interrogated the role of the vagus nerve in peripheral CCK- and meal-induced HPCd ACh responses in rats with either sham or sub-diaphragmatic vagotomy surgery (SDV) to disconnect GI vagus nerve signaling from the central nervous system (Fig. 4a, b). Elevations in HPCd ACh release from peripheral administration of CCK were observed in sham control rats. Meanwhile, this elevation was not observed in rats that received an SDV (Fig. 4c–e). Additionally, elevations in HPCd ACh release during active consumption of chow, as well as the sustained elevation of cholinergic tone in the satiated vs fasted state, were replicated in sham control rats. However, SDV abolished meal-induced ΔHPCd ACh release during active consumption, as well as the sustained elevation in cholinergic tone after voluntary meal termination without influencing the amount of food consumed (representative photometry traces in Fig. 4f, g; group compiled data in Fig. 4h–j). Meal period analyses of ΔHPCd ACh release in sham rats during active consumption revealed that cholinergic responses were higher in magnitude during later bouts compared to earlier ones only in sham controls, but not in SDV rats (Supplementary Fig. 4b–e). We next performed Western blot analyses in the HPC to quantify levels of proteins associated with ACh signaling, including choline acetyltransferase (ChAT), an enzyme that synthesizes ACh using choline and acetyl-CoA as precursors; vesicular acetylcholine transporter (VAChT), which carries ACh in vesicles for subsequent release upon synapse events, and acetylcholinesterase (AChE), an enzyme that degrades ACh after its release at the synaptic cleft. Results revealed that the SDV surgery significantly reduced VAChT levels in the HPCd compared to sham surgery (Fig. 4l), with no group differences in ChAT or AChE expression (Fig. 4k–m). These results indicate that gut vagus nerve ablation induces a reduction in ACh vesicular transport in the HPCd, without eliciting any compensatory changes in the expression of other proteins involved in ACh neurotransmission. Overall, these data indicate that the vagus nerve is required for dynamic HPCd ACh responses to gut-derived signals such as CCK and meal consumption, and that loss of vagal gut-brain signaling dampens HPCd ACh tone.

Western diet consumption blunts meal-induced hippocampal acetylcholine responses and CCK's satiating effects

Given that Western diet (WD) consumption is associated with both impaired hippocampal-dependent memory and blunted vagal gut-to-brain responses[20,21,23–25,36,37], we next assessed whether early-life WD diet consumption impacts meal-induced HPCd ACh responses and satiation responses to CCK. Animals were exposed to a cafeteria-style (CAF) WD for 30 days starting from postnatal day (PN) 26 and then switched to a standard chow diet prior to experimental testing from PN 60-85 (Fig. 5a). Consistent with previous studies from our laboratory[20,23,38,39] early life WD exposure did not affect body weights relative to standard chow fed animals (Supplementary Fig. 5a). Fiber photometry recordings during meal consumption (representative animal traces in Fig. 5b, c) revealed that early life exposure to a WD spared ΔHPCd ACh release elevations during active eating periods (Fig. 5e). However, fasted vs satiated analyses revealed that, unlike controls, CAF animals did not experience a sustained elevation in HPCd ACh release after voluntary meal termination (Fig. 5f) despite having consumed comparable amounts during the session (Fig. 5d). Furthermore, meal period analyses revealed controls but not CAF animals showed elevated magnitude of

https://doi.org/10.1038/s41467-026-73896-2

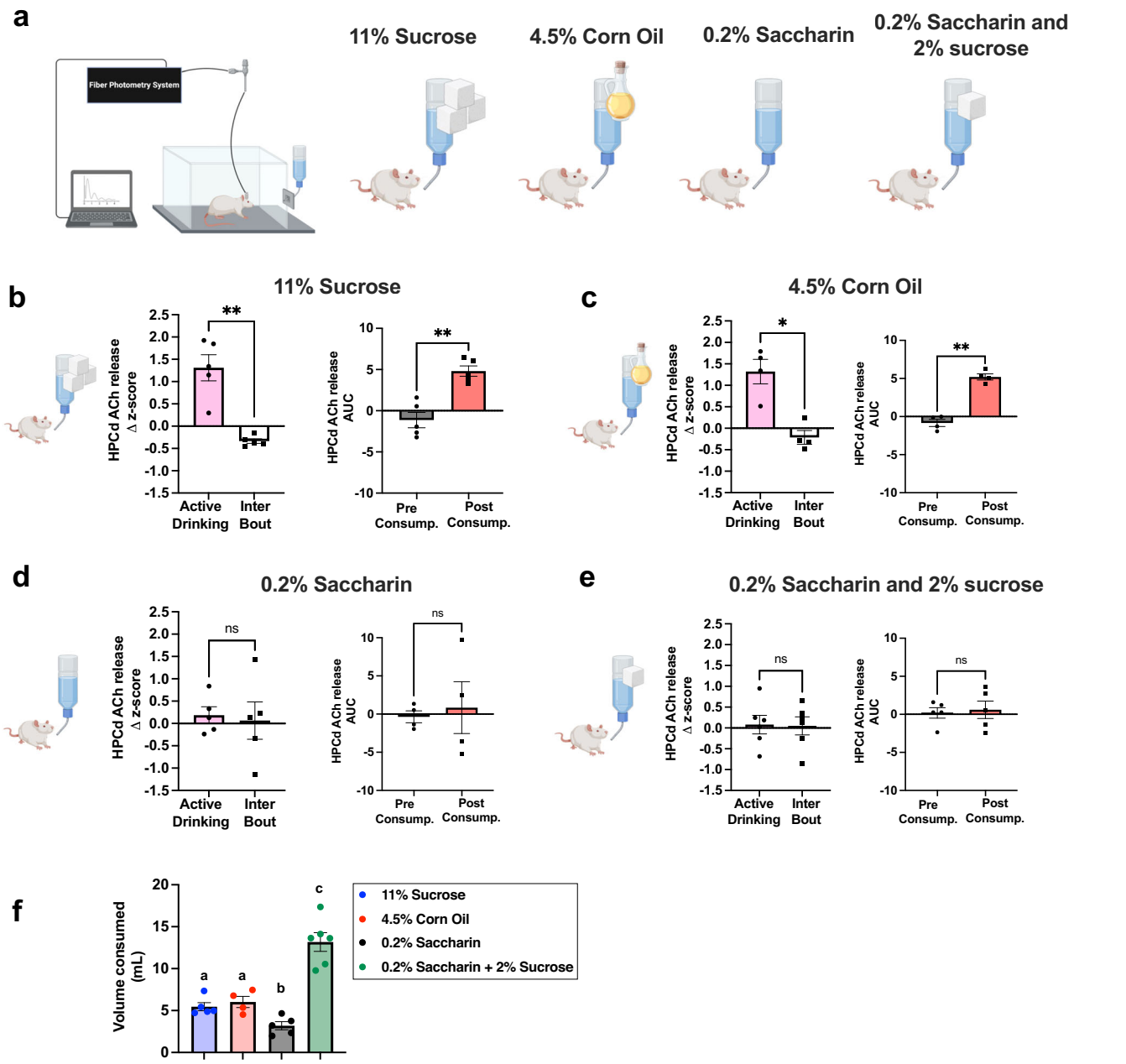

Fig. 3 | Meal-induced septo-hippocampal cholinergic signaling is driven by nutrients. a Schematic of fiber photometry recordings of HPCd ACh release during consumption of select isolated macronutrients or artificial sweetener in solution (created in BioRender. Kanoski, S. (2026) https://BioRender.com/oct60pn). **b**–**e** Fiber photometry recording of HPCd ACh release quantification during isolated macronutrient meal consumption (data analyzed using Student's two-tailed paired *t*-test) with **b** reflecting the comparison between the change in HPCd ACh release during active eating periods vs. inter bout intervals during 11% sucrose consumption: $n = 5$ rats, $^{**}P = 0.0032$, as well as the AUC comparison between pre-consumption and post-consumption periods $^{**}P = 0.0020$. **c** Change in HPCd ACh release during active eating periods vs. inter bout intervals during 4.5% corn oil consumption: $n = 4$ rats, $^{*}P = 0.0406$, as well as the AUC comparison between pre-consumption and post-consumption periods $^{**}P = 0.0046$. **d** Change in HPCd ACh release during active eating periods vs. inter bout intervals during 0.2% saccharin consumption: $n = 5$ rats, as well as the AUC comparison between pre-consumption and post-consumption periods. **e** Change in HPCd ACh release during active eating periods vs. inter bout intervals during 0.2% saccharin + 2% sucrose consumption: $n = 6$ rats, as well as the AUC comparison between pre-consumption and post-consumption periods. **f** Amount of isolated macronutrient/sweetener solution that was consumed during fiber photometry recording sessions. All treatment data containing the same letter are not significantly different (11% sucrose $n = 5$ rats vs. 0.2% saccharin $n = 5$ rats $^{*}P = 0.0223$, 11% sucrose vs. 0.2% saccharin + 2% sucrose $^{***}P = 0.0002$, 4.5% corn oil $n = 4$ rats vs. 0.2% saccharin $n = 5$ rats $^{**}P = 0.0096$, 4.5% corn oil vs. 0.2% saccharin + 2% sucrose $n = 6$ rats $^{**}P = 0.0014$, 0.2% saccharin vs. 0.2% saccharin + 2% sucrose $^{****}P = 0.000048$. Data are shown as mean ± SEM; $^{****}P < 0.0001$, $^{**}P < 0.01$. Source data are provided as a Source Data file.

ΔHPCd ACh release during late vs. early eating bouts (Supplementary Fig. 5b–e). To examine the long-lasting impacts of our early-life CAF WD model on vagal afferent nerve-mediated satiation signaling, we performed CCK food intake analyses during the healthy diet access period where fasted animals received either a low dose of CCK or vehicle IP, and chow intake was measured 30- and 60-min after. Results revealed that IP CCK (0.5 µg/kg) significantly reduced food intake at 30-min in animals raised on a standard chow diet, whereas CAF animals did not display reductions in food intake from IP CCK treatments at either time-point (Fig. 5g). Additionally, automated-home cage food intake measurements

https://doi.org/10.1038/s41467-026-73896-2

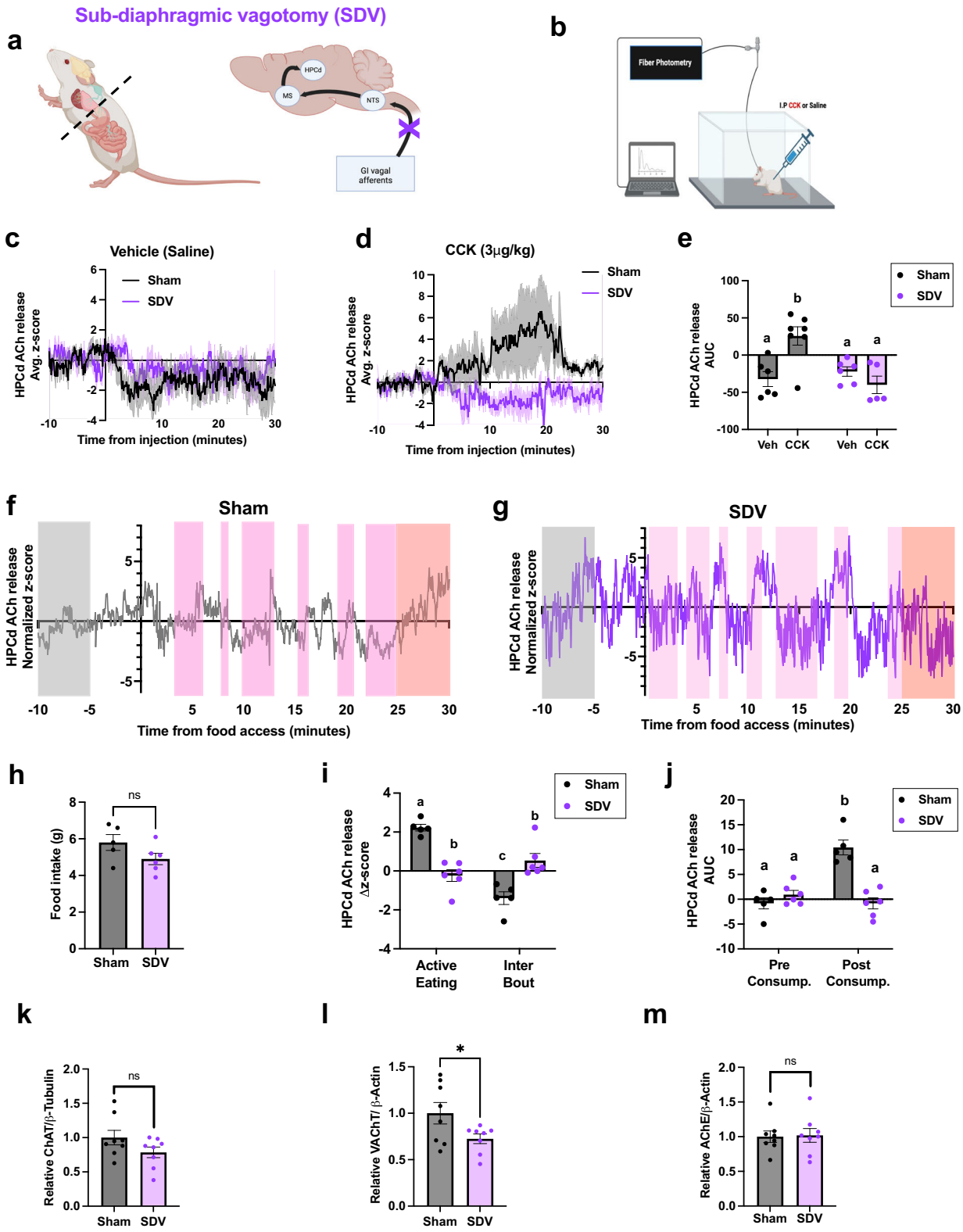

revealed that early-life CAF animals consumed significantly more food (chow) on average over a 6-day period than their control counterparts (Fig. 5h, i), and that this effect was driven by an increase in the average size of meals collapsed over the 6-day period (Fig. 5j–l). In summary, these results reveal that early-life WD exposure blunts vagally-mediated HPCd ACh responses to meal consumption, as well as the satiating response to a vagally-mediated dose of peripheral CCK well into adulthood. Thus, it is plausible that these impairments in vagus-brain signaling underlie hippocampal-dependent memory impairments associated with WD consumption.

Episodic memory for a meal requires the vagus nerve and septal cholinergic neurons, and is impaired by Western diet consumption

To determine the effects of the experimental models used in this study on meal-associated hippocampal-dependent memory performance,

Fig. 4 | Meal-induced septo-hippocampal cholinergic signaling requires the vagus nerve. a Schematic of subdiaphragmic vagotomy (SDV) (created in BioRender. Kanoski, S. (2026) https://BioRender.com/oeq264k). **b** Schematic of intraperitoneal administration of CCK during fiber photometry recording (created in BioRender. Kanoski, S. (2026) https://BioRender.com/8m1exlr). **c** Time-locked averaged HPCd ACh release to IP vehicle administration ($n = 6$ Vehicle-Sham; $n = 6$ Vehicle-SDV). **d** Time-locked averaged HPCd ACh release to IP CCK (3 µg/kg) administration ($n = 6$ CCK-Sham; $n = 6$ CCK-SDV). **e** HPCd ACh release AUC quantification in response to IP vehicle and CCK administration. Treatment data with the same letter above are not significantly different. Data were analyzed using two-way ANOVA with multiple comparisons; IP Treatment x SDV interaction $^{*}P = 0.0398$; Sham-Veh ($n = 6$ rats) vs. CCK ($n = 7$ rats) $^{**}P = 0.0071$; CCK treatment Sham ($n = 7$ rats) vs. SDV ($n = 5$ rats) $^{***}P = 0.0005$. **f**, **g** Representative trace of Sham (**f**) and SDV (**g**) rat HPCd ACh release during consumption of standard chow, time locked to the moment of access to food. Pre-consumption period (fasted state) is marked in the gray box, active eating periods [pink boxes; quantified as the Δ in activity between start and end of eating bout], inter bout intervals [white boxes; quantified as the Δ in activity between after the end of an eating bout and before the beginning of the subsequent eating bout], and post-consumption period (satiated state) marked in the red box are represented. **h** Food intake during fiber photometry recording sessions (Sham $n = 5$ rats; SDV $n = 6$ rats). Data analyzed using an unpaired two-tailed student's *t*-test. **i**, **j** Fiber photometry recordings of HPCd ACh release during food consumption in animals with either sham surgery (Sham; gray; $n = 5$ rats), or SDV (purple; $n = 6$ rats). All treatment data containing the same letter above are not significantly different; data were analyzed using two-way ANOVA with multiple comparisons (see "Statistical methods"), ($n = 5$, Sham; $n = 6$, SDV) with **i** depicting change in ACh release during active eating bouts and inter bout intervals for both experimental groups. SDV treatment x eating period interaction $^{****}P = 0.00005$. Sham, active eating vs. inter bout $^{****}P = 0.000074$; Active eating, Sham vs. SDV $^{****}P = 0.00001$; Inter bout, Sham vs. SDV $^{***}P = 0.0006$. **j** HPCd ACh release AUC quantification during pre-consumption and post-consumption periods. SDV treatment x energy state interaction $^{**}P = 0.0073$. Sham, pre consumption vs. post consumption $^{***}P = 0.00017$; Post consumption, Sham vs. SDV $^{***}P = 0.0002$. **k** Results for choline acetyltransferase (ChAT) protein levels in the HPCd of rats following sham or SDV surgery ($n = 8$, Sham; $n = 8$, SDV; paired two-tailed student's *t*-test, $P = 0.125$). **l** Immunoblot representative images and results for vesicular acetylcholine transporter (VAChT) protein levels in the HPCd of rats following sham or SDV surgery ($n = 8$, Sham; $n = 8$, SDV; paired two-tailed student's *t*-test, $P = 0.0154$). **m** Immunoblot representative images and results for acetylcholinesterase (AChE) protein levels in the HPCd of rats following sham or SDV surgery ($n = 8$, Sham; $n = 8$, SDV; paired two-tailed student's *t*-test, $P = 0.888$). $^{*}P < 0.05$. Data are shown as mean ± SEM. Source data are provided as a Source Data file.

animals were subjected to our "meal place recognition" procedure, which assesses working memory for the spatial location of recent eating. In this procedure, hungry rats consumed food in a hidden tunnel in a Barne's maze, and were then given a second trial shortly thereafter to test for food location memory (Fig. 6a). Memory probe test performance results revealed that animals injected with 192IgG saporin in the MS, SDV, or CAF animals had meal location-associated memory impairments, evidenced by their learning index within the probe test being significantly lower than that of their control counterparts (Fig. 6b–d). Further, while 192IgG saporin and SDV animals performed significantly worse than control saporin and sham animals, respectively, they also did not perform better than chance. Although CAF animals underperformed relative to their control counterparts, their performance was significantly above chance (Fig. 6d), suggesting that early-life CAF diet blunts gut-vagal-hippocampus signaling, but to a lesser degree than ablation of the vagus nerve or MS ACh neurons.

To interrogate how HPCd ACh release is engaged during this food-motivated spatial memory task, as well as whether memory test recruitment of ACh signaling requires the vagus nerve, we performed recordings of ACh release in sham and SDV animals during the memory probe test. Similar to Fig. 6c, memory deficits were replicated in SDV vs. sham rats (Supplementary Fig. 6a). Quantification of ACh release during and 3 s after hole investigations in sham control rats revealed that ACh release in the HPCd was significantly higher upon correct vs. incorrect hole investigations, in terms of the max z-score of ACh release reached, but not the AUC of HPCd ACh release (Fig. 6g, h). In SDV animals, however, there were no significant differences based on correct vs. incorrect hole for either ACh measure (Fig. 6g, h). When directly comparing groups for each type of hole investigation, AUC was significantly higher in the sham group for correct but not incorrect hole investigations, whereas the maximum *z*-score of ACh release was significantly higher in the sham group for both correct and incorrect investigations compared to SDV animals (Fig. 6g, h). Given that hippocampal ACh has previously been associated with animal movement speed during navigation[40,41], we sought to understand whether this association is observed in the food-motivated spatial memory, and whether SDV affects ACh-speed coupling by performing a linear regression of the coupling between changes in locomotor speed and changes in HPCd ACh release. Results reveal that average locomotor speed did not differ between sham and SDV groups (Supplementary Fig. 6b), nor did we observe a consistent coupling between concurrent changes in speed and ACh release in sham or SDV animals (Supplementary Fig. 6c, d). Together, these data identify memory impairments in the location of a recently consumed meal across three distinct yet related experimental models that disrupt HPCd ACh responses to vagally mediated GI signals. Additionally, HPCd ACh release is engaged during a meal location working memory test in control but not SDV animals, thus further supporting a role between the vagus nerve, HPCd ACh release, and memory function.

Discussion

Despite recent findings implicating the vagus nerve in the modulation of cognitive processes[5,10], the neural substrates driving these phenomena, particularly promoting HPC-dependent memory function, remain poorly understood. Our findings establish a gut-brain substrate through which nutrient-induced activation of GI vagal afferent nerve (VAN) signaling engages HPCd ACh signaling via MS cholinergic neurons. This neuronal pathway is responsive to vagally-transmitted satiation signals, including CCK and physiological meal consumption, and is disrupted by early-life WD exposure. These data offer fundamental mechanistic insights into how peri-prandial physiological signals shape HPCd activity and thus contribute to our understanding of how interoceptive signals from the gut affect learning and memory processes.

Our results reveal that peripheral administration of CCK increases HPCd c-Fos expression and ACh signaling tone, effects that are abolished by either selective ablation of MS cholinergic neurons or by subdiaphragmatic vagotomy (SDV) treatment. This provides causal evidence that MS cholinergic neurons serve as a key relay for conveying vagal information to the HPCd, particularly the dorsal dentate gyrus (DG) and CA3 subfields. While the MS has been known to regulate hippocampal theta rhythm and memory encoding through its cholinergic output[42,43], our work identifies an upstream physiological GI influence on this circuit, mediated through GI VAN.

Impairments in meal-location memory were observed across all experimental models that disrupt vagal-ACh-HPCd communication—SDV, MS cholinergic ablation (192 IgG SAP) and early-life WD exposure. Given the established role of HPCd ACh transmission in memory encoding[16–18], and that WD-induced HPC impairments occur through dysregulation of ACh transmission[23], our data showing parallel disruptions in meal-associated HPCd ACh release in SDV and CAF animals (Figs. 4 and 5) provide evidence that a junk food diet and overall loss of integrity of VAN signaling yield memory impairments via disruptions in vagal-ACh-HPCd signaling. CAF animals exhibited

https://doi.org/10.1038/s41467-026-73896-2

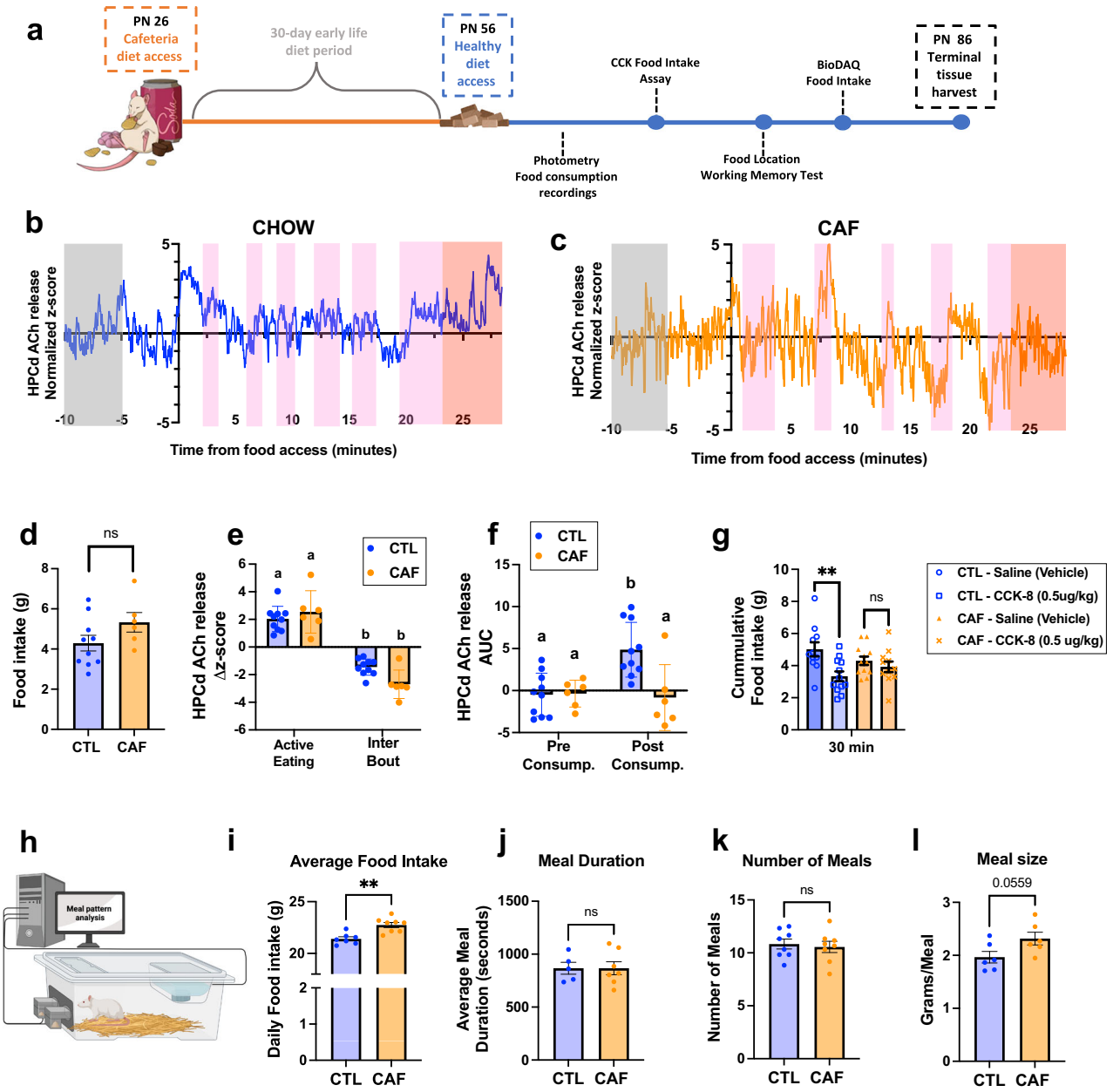

Fig. 5 | Western diet blunts gut-vagal signaling and eliminates meal-induced septo-hippocampal cholinergic responses. a Experimental design timeline for fiber photometry and behavioral assessments. **b**, **c** Representative trace of chow fed (**b**) and cafeteria (CAF) fed (**c**) rats HPCd ACh release during consumption of standard chow, time locked to moment of access to food. Pre-consumption period (fasted state) is marked in the gray box, active eating periods [pink boxes; quantified as the Δ in activity between start and end of eating bout], inter bout intervals [white boxes; quantified as the Δ in activity between after the end of an eating bout and before the beginning of the subsequent eating bout], and post-consumption period (satiated state) marked in the red box are represented. **d** Standard chow intake during fiber photometry recording sessions (CTL $n = 10$ rats; CAF $n = 6$ rats). Data analyzed using an unpaired two-tailed student's *t*-test. **e**, **f** Fiber photometry recordings of HPCd ACh release during food consumption in control (chow fed; CTL) and CAF animals (CTL; blue), or CAF (orange). All treatment data containing the same letter above are not significantly different; data were analyzed using two-way ANOVA with multiple comparisons (see "Statistical methods"), ($n = 10$, CTL; $n = 6$, CAF) with e. depicting change in ACh release during active eating bouts and inter bout intervals for both experimental groups. Diet treatment x eating period interaction $P = 0.239$. CTL, active eating vs. inter bout $^{****}P = 0.00008$; CAF, active eating vs. inter bout $^{****}P = 0.00004$; Active eating, CTL vs. CAF $P = 0.635$; Inter bout, CTL vs. CAF $P = 0.0593$. f. HPCd ACh release AUC quantification during pre-consumption and post-consumption periods. Diet treatment x energy state interaction $^{*}P = 0.0116$. CTL, pre-consumption vs. post-consumption$^{***}P = 0.0007$; Post-consumption, CTL vs. CAF $^{**}P = 0.0017$. **g** 30-min cumulative standard chow intake of CTL and CAF rats after IP saline (vehicle) or CCK (0.5 µg/kg). All treatment data containing the same letter above are not significantly different; data were analyzed using two-way ANOVA with multiple comparisons (see "Statistical methods"), ($n = 12$, CTL; $n = 12$, CAF). Diet x IP Treatment interaction $P = 0.1534$. CTL, vehicle vs. CCK $^{**}P = 0.0063$; CAF, vehicle vs. CCK $P = 0.2786$; Vehicle, CTL vs. CAF $P = 0.7546$; CCK, CTL vs. CAF $P = 0.4754$. **h** Schematic of rats in the BIODAQ system for automated meal pattern analyses (created in BioRender. Kanoski, S. (2026) https://BioRender.com/ojjdxkm). **i** Average daily food intake over 6-day period in CTL ($n = 7$) and CAF animals ($n = 8$) $^{**}P = 0.0011$. Data analyzed using an unpaired two-tailed student's *t*-test. **j** Average daily meal duration in seconds, (CTL $n = 7$; CAF $n = 8$) $P = 0.9985$. Data analyzed using an unpaired two-tailed student's *t*-test. **k** Average daily number of meals, (CTL $n = 7$; CAF $n = 8$) $P = 0.7063$. Data analyzed using an unpaired two-tailed student's *t*-test. **l** Average daily meal size expressed as grams per meal (CTL $n = 7$; CAF $n = 8$) $P = 0.0559$. $^{**}P = 0.0063$. Data analyzed using an unpaired two-tailed student's *t*-test. Data are shown as mean ± SEM. Source data are provided as a Source Data file.

https://doi.org/10.1038/s41467-026-73896-2

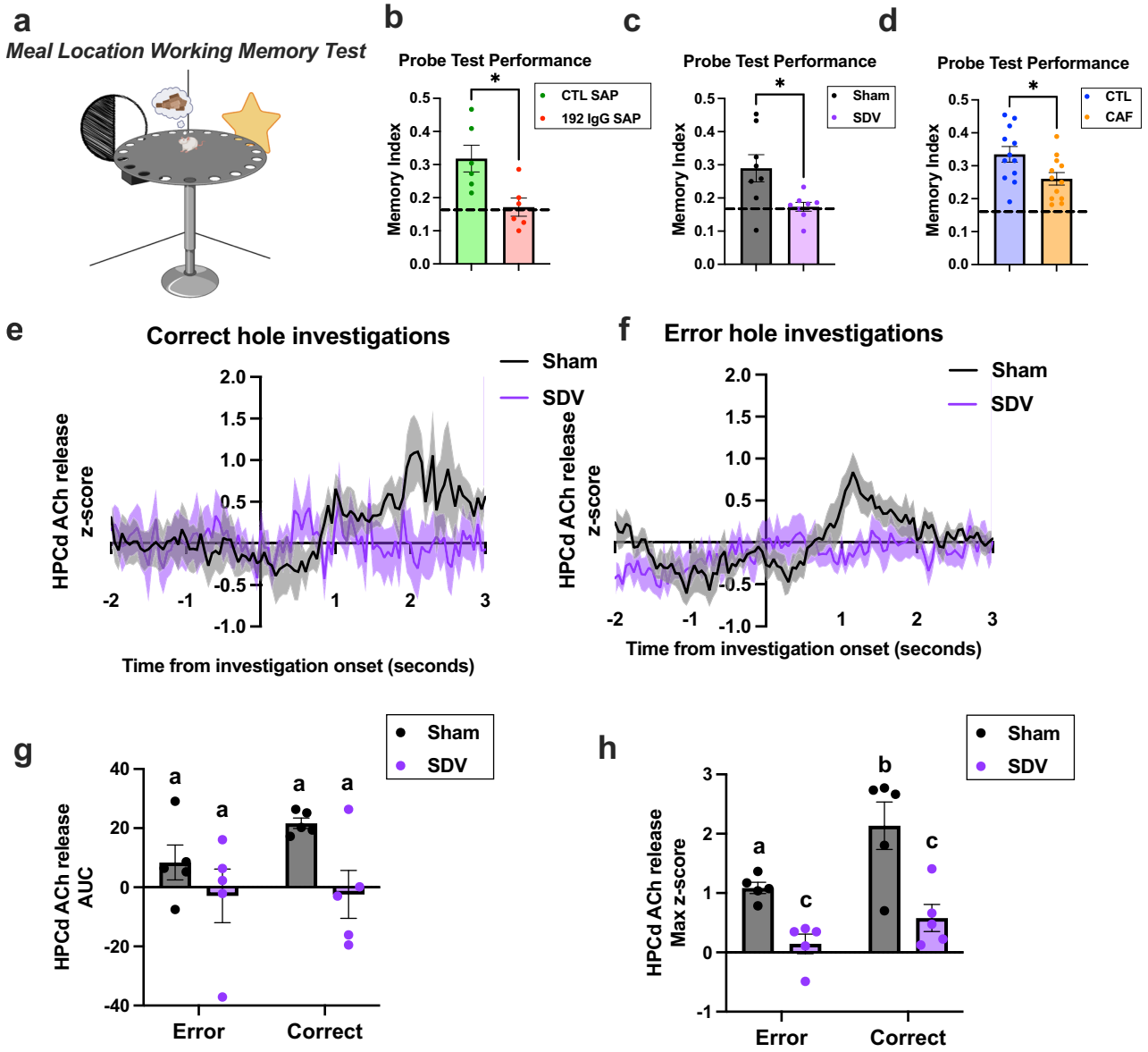

Fig. 6 | Hippocampal cholinergic signaling during food location working memory performance depends on intact vagal input. a Schematic of Meal Location Working Memory Paradigm (created in BioRender. Kanoski, S. (2026) https://BioRender.com/5vog18n). **b** Memory performance during probe test (expressed as learning index) in animals with control saporin in the MS (CTL SAP; green) or 192IgG SAP (red) in the MS; ($n = 6$, CTL SAP; $n = 6$ 192IgG SAP) CTL SAP vs. 192IgG SAP $^*P = 0.134$; CTL SAP null hypothesis test $^*P = 0.0135$; 192IgG SAP null hypothesis test $P = 0.8681$. Data analyzed using an paired two-tailed student's *t*-test, and null hypotheses were tested using one sample *t*-tests against 0.16 as the null value. **c** Memory performance during probe test (expressed as memory index) in animals that received either sham surgery (sham; gray) or SDV (purple); ($n = 8$, Sham; $n = 8$ SDV) Sham vs. SDV $^*P = 0.0379$; Sham null hypothesis test $^*P = 0.0200$; SDV null hypothesis test $P = 0.6287$. Data analyzed using an unpaired two-tailed student's *t*-test, and null hypotheses were tested using one sample *t*-tests against 0.16 as the null value. **d** Memory performance during probe test (expressed as learning index) in chow fed (CTL; blue) animals or CAF fed animals (orange); ($n = 12$, CTL; $n = 12$, CAF) CTL vs. CAF $^*P = 0.0233$; CTL null hypothesis test $^{****}P = 0.00002$; CAF null hypothesis test $^{***}P = 0.0005$. Data analyzed using an paired two-tailed student's *t*-test, and null hypotheses were tested using one sample *t*-tests against 0.16 as the null value. **e** Time-locked average z-score of HPCd ACh release during correct hole investigations and error hole investigations **f** in sham ($n = 6$; black) and SDV ($n = 6$; purple) animals. All treatment data containing the same letter above are not significantly different; data were analyzed using a two-way ANOVA with multiple comparisons (see "Statistical methods"), with **g** depicting HPCd ACh release AUC over 3 s post correct and error hole investigations. SDV Treatment x Investigation Type $P = 0.5239$; Sham correct vs error $P = 0.5960$; Correct Sham vs. SDV $P = 0.2559$; Sham correct null-hypothesis $^{***}P = 0.0002$; Sham error null-hypothesis $P = 0.2280$ (Sham $n = 5$; SDV $n = 5$). **h** HPCd ACh release max *z*-score reached within 3 s post investigation of correct vs. error hole investigations. SDV Treatment x Investigation Type interaction $P = 0.0935$; Sham correct vs. error $^*P = 0.0122$; Correct Sham vs. SDV $^{**}P = 0.0028$; Error Sham vs. SDV $^*P = 0.0177$; Sham Correct null-hypothesis $^{**}P = 0.0060$; Sham Error null-hypothesis $^*P = 0.0248$; SDV Correct null-hypothesis $P = 0.0640$ (Sham $n = 5$; SDV $n = 5$). Data were analyzed using a two-way ANOVA with multiple comparisons (see "Statistical methods"). Data are shown as mean ± SEM. Source data are provided as a Source Data file.

milder memory deficits compared to vagotomized or MS ACh neuron-ablated rats, which may reflect the preservation of short-timescale cholinergic dynamics during active consumption and inter-bout intervals in these animals. This suggests that temporally-specific ACh signaling during eating may contribute to HPC memory function and that compensatory mechanisms and/or persistence of other HPC inputs may partially offset vagal dysfunction in diet-exposed animals. Nonetheless, the consistency across models – with regards to both impairments in HPC-dependent spatial memory and post-meal-induced elevations in ACh release – underscores the critical role of

vagal-ACh-HPCd signaling in encoding episodic memories related to eating events.

Fiber photometry recordings reveal robust and temporally structured increases in HPCd ACh release during active eating bouts, particularly during later phases of the meal and following meal termination. Analyses of within- and between-bout dynamics uncovered a consistent alignment between ACh fluctuations and behavioral state transitions, as the slope of ACh release shifted almost immediately upon behavioral transitions – upwards after an eating bout started and downwards after a bout terminated. These temporal relationships suggest that HPCd ACh signaling is rapidly modulated by behavioral transitions between consummatory and non-consummatory states. These findings are consistent with previous research identifying ACh HPCd signaling in attention reallocation, contextual encoding, and behavioral flexibility[16,44,45]. The relative suppression of ACh release during interbout intervals may also reflect transient disengagement of VAN firing during pauses in ingestion, and/or involvement of inhibitory circuits that temporarily reduce MS ACh-> HPCd to facilitate other HPC processes, such as sharp wave ripple events[41]. Notably, the effects of CCK on HPCd ACh release, which require both cholinergic MS neurons and VAN signaling, were not observed with another gut-derived satiation peptide, amylin, that exerts its anorectic effects independently of vagal transmission[32]. These findings highlight vagally-mediated physiological nutrient signaling as a key regulator of HPCd neurophysiology, and that these responses are dynamically and instantly modulated by behavioral transitions during eating.

In dissecting the drivers of meal-induced ACh release, we show that caloric nutrients (sucrose and corn oil) elicit significant HPCd ACh responses, while non- and low-nutritive sweeteners (saccharin, or saccharin + 2% sucrose) do not, despite comparable palatability and higher ingestion volumes in the latter condition. This nutrient-dependence suggests that HPCd cholinergic activation requires post-ingestive signaling—likely involving GI nutrient-sensing mechanisms (e.g., nutrient receptors, enteroendocrine cells) that act upstream of vagal afferents[28,46]. Furthermore, previous work has shown that nutrient sensing in the gut engages vagal circuits to drive behavior and affect central nervous system function[33,47]. Our data expands this concept by identifying HPCd cholinergic tone as a sensitive index of gut-nutrient detection and by implicating this system in the encoding of meal-related memory processes. Furthermore, given that HPCd ACh responses are identical between pure lipid and carbohydrate ingestion, it is likely that ACh signaling in the HPCd is not responsible for the recently reported recruitment of separate HPC ensembles associated with fats and sugars[12]. Therefore, while HPCd ACh is involved in encoding spatial information relevant to nutritive consumption, other pathways likely contribute to the recruitment of HPC ensembles that represent the consumption of different macronutrients.

The temporal dynamics of HPCd ACh release observed during and after a meal are broadly consistent with the known activation profiles of GI vagal afferent pathways. Nutrient detection in the small intestines rapidly engages VANs via CCK1 receptor (CCKR +)-dependent mechanisms and glutamatergic transmission from enteroendocrine neuropod cells[48]. Similarly, peripheral CCK administration elicits calcium responses in the nodose ganglia neurons on the timescale of seconds to minutes[49], and CCK-sensitive C-type vagal afferents activate neurons in the medial nucleus of the solitary tract (mNTS) within milliseconds to seconds[50]. Similarly, studies have reported rapid responses (within milliseconds to seconds) of VANs that respond to gastric distension[51,52]. Together, these findings support a model in which CCK- and distension-responsive vagal afferents provide a rapid and sustained excitatory drive that accounts for the elevation of HPCd ACh observed during active eating bouts. On the other hand, the persistence of elevated HPCd ACh release following meal termination likely reflects continued engagement of late-meal and/or post-ingestive vagal signaling as nutrients progress through the intestines, rather than a simple accumulation of signals across discrete feeding bouts. Notably, while CCK signaling is strongest during proximal intestinal nutrient detection, other vagal pathways may contribute to later phases of cholinergic activation. Glucagon-like peptide-1 (GLP-1), for example, is released from distal intestinal L-cells and modulates eating and glycemic control through vagal mechanisms[53–55]. Thus, we hypothesize that GLP-1 signaling contributes to the sustained post-prandial HPCd ACh elevations in conjunction with CCK, whereas the rapid cholinergic responses observed during individual feeding bouts are mediated by both rapid CCK and gastric distension signaling. While this hypothesis will require additional investigation to confirm, our confidence in a primary role for CCKR+ VANs in driving HPCd ACh release is grounded from our previous results revealing that ablation of CCKR+ VANs replicated the HPC-dependent memory impairments (and reductions in neurogenic and neurotrophic markers) observed in SDV rats[10], combined with presents results showing that a dose of peripheral CCK that requires VAN for effects on food intake drives HPCd ACh release in controls, but not in vagotomized rats.

Consistent with previous findings[19–23,36,39], early-life consumption of a WD impaired hippocampal-dependent memory, even following healthy diet intervention at adult onset. Building on this work, here we show that early-life WD also abolished sustained elevations in post-meal HPCd ACh signaling. These signaling deficits were accompanied by blunted anorexigenic responses to peripheral CCK administration and increased average spontaneous meal size, suggesting a functional disconnection between vagal satiation signals and hippocampal memory systems following early-life WD. Mechanistically, these impairments may stem from WD-induced gut barrier dysfunction, microbiome shifts, and/or VAN remodeling[20,56], which have been associated with diminished gut-to-hindbrain communication.

Chronic reductions in ACh signaling markers from early-life CAF diet (e.g., VAChT, parallel to those seen in SDV here) are linked with disruptions in HPCd ACh signaling during object-context novelty recognition[23]. In this previous study from our lab, investigation of an object that is novel to a specific context elicits robust increases in HPCd ACh release in control animals, but this effect is absent in CAF animals and is accompanied by their impairments in memory performance. Notably, these behavioral deficits are rescued by direct HPCd infusions of a cholinergic (ACh α7 nicotinic) receptor agonist delivered during the encoding phase of the task[23], highlighting both the necessity of intact cholinergic signaling for HPC-dependent memory formation, and the HPCd cholinergic dysfunction in this early life WD model. Based on these findings, we propose that meal-induced elevations in HPCd ACh may have evolved to encode contextual and spatial information related to food acquisition to facilitate efficient future foraging, but that this system may also have an ancillary function for contextual learning absent food consumption. Importantly, the reductions in HPCd VAChT expression following SDV (present study) and Western diet exposure[23] (our previous study), in both cases without compensatory changes in choline-acetyl transferase (ChAT) or acetylcholinesterase (AChE) expression, may reflect a synaptic adaptation to diminished vagal-driven MS ACh->HPC signaling, wherein reduced recruitment of MS cholinergic neurons lowers the demand for VAChT-mediated vesicular ACh trafficking and release capacity. Beyond these neural mechanisms, diet-induced disruptions of vagal-ACh-HPCd signaling may also exert long-lasting effects through non-neuronal pathways, as ACh acting on α7 nicotinic receptors on microglia and astrocytes confers anti-inflammatory actions that are critical to maintaining HPC integrity and cognitive function[57–59].

HPCd ACh signaling is engaged under conditions of novelty, uncertainty, and memory updating[44,60,61]. Consistent with this framework, we revealed that HPCd ACh release is selectively enhanced during correct vs. incorrect meal location investigations in sham animals, but not in SDV animals, in a memory probe test where the previously reinforced meal consumption tunnel is no longer

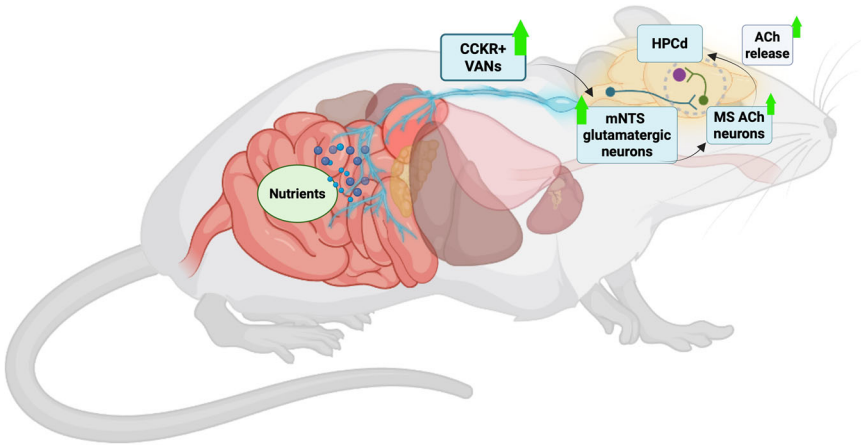

Fig. 7 | Model for nutrient-induced modulation of hippocampal function. Created in BioRender. Kanoski, S. (2026) https://BioRender.com/gd4kds1.

available. This dissociation is not explained by differences in locomotor variables, as neither average speed nor moment-to-moment speed-ACh coupling differed significantly between groups. Rather, these data indicate that HPCd ACh signaling is preferentially recruited during memory-relevant sampling events that require updating of spatial representations during extinction learning, and that these responses require the vagus nerve. Consistent with these findings, HPCd ACh signaling increases during early extinction and contingency updating, reflecting the engagement of encoding mechanisms rather than retrieval[62–65].

Our findings build upon and extend recent work from our group demonstrating that ventral hippocampal (HPCv) circuits contribute to food-related spatial cognition via downstream interactions with the lateral hypothalamic area (LHA). In a spatial reference memory version of the Barnes maze where the food location remains stable across days, HPCv output and serotonin (5-HT2A) signaling regulated memory task performance and motivational aspects of food investigation and consumption[66]. In contrast, the present study employed a working memory variant of the meal location task, in which the escape hole location changes daily and must be encoded and retrieved on a short-term trial-by-trial basis. This task places greater demands on rapid spatial encoding, flexible updating, and precise temporal alignment between neural activity and behavior—functions that are classically associated with the HPCd. On the other hand, spatial reference memory for food location, based on our previous work, appears to be mediated by the HPCv[10,66]. These differences are consistent with the well-established functional gradient along the longitudinal hippocampal dorsal-ventral / anterior-posterior / septo-temporal axis. The HPCd is specialized for fine-grained spatial representations and rapid, event-linked encoding, whereas the HPCv operates over broader spatial and temporal scales, integrating motivational, emotional, and interoceptive signals[67–72]. Within this framework, vagal afferent input may regulate both hippocampal subregions, but through distinct signaling mechanisms. Rapid vagal firing driven by proximal nutrient detection—such as CCK-sensitive afferent pathways—may preferentially engage septal-hippocampal cholinergic signaling to the HPCd, supporting fast, trial-specific memory updating.

Our results do not suggest that ACh acts in isolation. Rather, the present findings, combined with previous published work, support a model in which multiple neuromodulatory systems (e.g., ACh, serotonin, norepinephrine) interact across hippocampal subregions to support food-related learning and memory, with the relative contribution of each system determined by task structure and temporal demands. The present data clearly identify vagal-dependent HPCd ACh signaling as a critical component for spatial working memory for food location, while our prior work highlights complementary roles for HPCv circuits and monoaminergic signaling for food location reference memory and consummatory control. Together, these studies suggest a coordinated, region-specific framework in which vagal input and humoral signals differentially engage hippocampal subregions to regulate food-based memory and consumption.

The work presented here offers mechanistic insight into how signals from the gut modulate the septo-hippocampal memory system and how this signaling pathway responds to unhealthy dietary insults. Based on present data, existing neuroanatomical evidence, and prior functional studies, our working model presented herein is that GI vagal afferent neurons are activated by nutritive signals—particularly CCK released during meal consumption—and excite glutamatergic neurons within the medial nucleus of the solitary tract of the brainstem (mNTS), the site where VANs directly synapse into the brain. These mNTS neurons, in turn, provide excitatory input to medial septal (MS) cholinergic neurons, leading to elevated acetylcholine (ACh) release in the HPC (Fig. 7).

Present results call for clinical research endeavors to investigate this system in the context of neurodegenerative disorders such as Alzheimer's Disease (AD), given the established literature showing that AD is characterized by deterioration of the HPC cholinergic signaling[73], and may be linked with vagus nerve ablation. Taken together with recent emerging findings, collective results demonstrate that dietary insults yield HPC ACh dysregulation parallel to those seen in AD, and thus support the need for future investigation into the links between obesogenic early-life diets and subsequent development of AD[74–76]. Consistent with this framework, a population-based cohort study of patients who received a vagotomy as a form of treatment for gastric ulcers in Taiwan demonstrated a significantly higher risk of developing dementia in vatomized individuals vs. control-matched individuals[77]. These findings further highlight the translational importance of the vagus-ACh-HPC circuitry studied here in the context of diet-induced cognitive impairments and AD etiology, and align with the existing literature demonstrating the potential benefits of vagus nerve stimulation on dysregulated memory function[5,8,78,79]. Therapeutic strategies aimed at restoring vagal tone and/or enhancing septo-hippocampal cholinergic signaling may thus offer novel avenues for treating obesity-, dietary-, environmental-, and/or genetic-mediated memory impairments.

Methods

Animals

Male Sprague–Dawley rats (Envigo; 300–400 g; and 70–90 g for CAF diet experiment on arrival) were individually housed with ad libitum access (except where noted) to water and chow (LabDiet 5001, LabDiet, St. Louis, MO) on 12 h:12 h light/dark cycle (lights on at 23:00 h).

All procedures involving animals were approved by the University of Southern California Institute of Animal Care and Use Committee.

Intracranial viral injection and in vivo photometry optic fiber placement

Rats were anesthetized and sedated via intramuscular injection of a ketamine (90.1 mg/kg), xylazine (2.8 mg/kg), and acepromazine (0.72 mg/kg) cocktail. This was followed by a preoperative subcutaneous injection of the analgesic buprenorphine SR (1.3 mg/kg). Once sedated, the surgical site was shaved and disinfected with iodine and ethanol swabbing before the animals were secured in a stereotaxic apparatus. Adeno-associated virus (AAV) encoding iAChSnFR (1 µL; original titer $\geq 7 \times 10^{12}$ vg/mL, diluted 1:2 in artificial cerebrospinal fluid; pAAV.hSynap.iAChSnFR, 137950-AAV1, Addgene, Watertown, MA, USA)—previously validated as a selective in vivo ACh sensor in rodents[80–83]—was injected bilaterally into the dorsal dentate gyrus of the hippocampus (HPCd) using a micro infusion pump (Harvard Apparatus, Cambridge, MA, USA) equipped with a 33-gauge micro syringe injector connected to a PE20 catheter and Hamilton syringe. The injection was delivered at a rate of 5 µL/min, with injectors left in place for an additional 2 min to ensure complete infusion. Following viral delivery, fiber optic cannulae (flat 400 µm core, 0.48 numerical aperture, 5 mm; Doric Lenses Inc., Quebec, Canada) were implanted at the same stereotaxic coordinates as the viral injection (A/P: −3.24; M/L: ±1.80; D/V: −3.50, with bregma as the reference point). The optic fibers were secured to the skull using jeweler's screws, instant adhesive super glue, and dental cement.

For medial septum cholinergic neuron ablation, the described preoperative methodology was repeated. The antineuronal immunotoxin 192IgG saporin, which has been validated as an agent that selectively ablates neurons that produce acetylcholine[10,84,85], was injected in the medial septum; 200nL (0.16 µg/µL) were infused in three different coordinates that span the medial septum (A/P_1: 0.5, M/L_1: 0.5, D/V_1: −7.4, A/P_2: 0.5, M/L_2: 0, D/V_2: −6.8, A/P_3: 0.5, M/L_3: −0.5, D/V_3: −7.4, with bregma as the reference point). Rats were allowed to recover after surgery for 2 weeks before the experiments proceeded.

In vivo fiber photometry

Fiber photometry signal acquisition was performed using the Neurophotometrics system (Neurophotometrics, San Diego, CA) at a sampling frequency of 40 Hz, with alternating excitation wavelengths of 470 nm (ACh-dependent) and 415 nm (ACh-independent). Fluorescence was transmitted through an optical patch cord (Doric Lenses) and directed onto the implanted optic fiber, which in turn relayed neural fluorescence back through the same optic fiber and patch cord to a photoreceiver. Behavioral events, including cues, entries, and eating bouts, were time-stamped using the data acquisition software (Bonsai). To correct for baseline neural activity and motion artifacts, the ACh-independent signal was subtracted from the ACh-dependent signal, and the resulting fluorescence fluctuations were fitted to a biexponential curve. The corrected fluorescence signal was then normalized for each rat by calculating $\Delta F/F$ using the average fluorescence signal from the entire recording, followed by conversion to z-scores. Finally, the normalized signal was aligned to relevant behavioral events, and data extraction was performed using custom MATLAB code.

Fiber photometry during meal consumption

Prior to the test day, rats underwent an overnight fast with *ad libitum* access to water. Testing occurred in the early nocturnal/dark phase for a 24-h period without food. On test days, animals were first placed in a neutral context (neutral rat cage in a procedure room with dim lighting) for 15 min without food, followed by a 30-min chow access period (Laboratory Rodent Diet 5001, St. Louis, MO, USA). Afterward, food was removed, and animals remained in the context for an additional 10 min. Eating bouts and inter bout intervals were manually time-stamped within the photometry data acquisition stream by an experimenter observing the animals eat on a video monitor system. Eating was defined as the time the animal began consuming food, and interbout intervals reflect the time the animal paused eating (no longer chewing or consuming food). To assess the effects of physiological HPCd ACh release during refeeding after an overnight fast, in vivo fiber photometry was performed. A patch cord was connected to the implanted optical fiber, and LEDs alternated between 470 nm (ACh-dependent) and 415 nm (ACh-independent) wavelengths throughout the task. The 5-min pre-consumption period for each animal was defined as a 5-min period terminating 5 min before food access. This pre-consumption period was defined a priori in order to avoid experimenter interference with the baseline signal at the time of food access delivery. The 5-min post-consumption period was defined as a 5-min period immediately after voluntary meal termination (5 min or longer without eating), or for animals who did not voluntarily terminate a meal with 30 min, it was defined as the 5-min period beginning 5 min after food removal. This post-meal period was defined a priori in order to avoid experimenter interference at the time of food removal.

Liquid meal consumption analyses were conducted under similar conditions, except that the consumption tests occurred in operant boxes with lickometers to deliver solutions (Med Associates Inc., Fairfax, VT). Additionally, the order of caloric (11% sucrose, and 4.5% corn oil) and non-caloric (0.2% saccharin and 0.2% saccharin + 2% sucrose) solutions given to the animals was fully counterbalanced.

Subdiaphragmatic vagotomy (SDV)

Animals were habituated to a liquid diet (Research Diets; AIN76A) for five days prior to surgery. Following a 24-h fast, surgeries were performed under anesthesia with ketamine (90.1 mg/kg), xylazine (2.8 mg/kg), and acepromazine (0.72 mg/kg), along with analgesia provided by Metacam (2 mg/kg). The trunks of the subdiaphragmatic vagus nerve were transected. A midline abdominal incision was made, after which the stomach was retracted caudally and the liver cranially to expose the esophagus. The dorsal and ventral branches of the vagus nerve were carefully dissected from the esophagus, ligated twice with surgical thread at 1–2 cm intervals, and then cauterized between the ligatures. In sham surgeries, the vagal trunks were exposed but neither ligated nor cauterized. The incision was closed using running sutures for the abdominal wall and stop sutures for the skin. Rats were allowed to recover until their liquid diet intake stabilized (a minimum of one week), after which they were transitioned back to a standard chow diet.

Dietary model

To simulate a Western "junk food" diet during early life, we implemented a junk food cafeteria-style (CAF) diet. This diet provided ad libitum access to a high-fat, high-sugar chow (HFHS diet; D12415, Research Diets, New Brunswick, NJ, USA; 20% kcal from protein, 35% kcal from carbohydrates, 45% kcal from fat), along with potato chips (Ruffles Original, Frito Lay, Casa Grande, AZ, USA), crushed up chocolate-covered peanut butter cups (Reese's Minis Unwrapped, The Hershey Company, Hershey, PA, USA), and an 11% weight/volume (w/v) high-fructose corn syrup-55 (HFCS) beverage (Best Flavors, Orange, CA, USA). Each food and drink item was placed in separate receptacles within the home cage. The 11% w/v HFCS concentration was selected to match the sugar content of commonly consumed sugar-sweetened beverages, as previously modeled. CAF-fed rats also had ad libitum access to water. Control (CTL) rats were provided with the same number of food and drink receptacles; however, these contained only standard chow (LabDiet 5001; LabDiet, St. Louis, MO, USA; 28.5% kcal from protein, 13.5% kcal from fat, 58.0% kcal from carbohydrates) and water. Body weight and food intake—including any spillage collected from cardboard placed beneath the hanging wire cages—were measured three times per week between 8:30 and 10:30 AM, just before the

onset of the dark cycle. For the CAF diet model experiments, juvenile rats arrived at the animal facilities on postnatal day (PN) 25. The subsequent day (PN 26), rats were randomly assigned to either the CAF or CTL group (n = 12 per group) and given ad libitum access to their respective diet. At PN 56, the CAF group of rats was switched to the 'healthy' standard chow diet (LabDiet 5001), the same diet as the CTL group. Experiments with this dietary model were performed after the CAF group had been switched to/acclimated to the 'healthy' standard chow diet (PN 63 +).

For meal pattern analyses, animals were housed in a BioDAQ food monitoring intake system (Research Diets Inc., New Brunswick, NJ) to which they were habituated for at least 5 days prior to any recordings. An inter-meal interval (IMI) of 900 s was used to separate individual eating bouts into separate meals. Cumulative chow intake and meal patterns were recorded for 6 consecutive days.

c-Fos protein expression

Surgically treated (MS saporin injections) rats ($n = 17$) received intraperitoneal (IP) injections of either saline ($n = 8$) or CCK (CCK-8, 3.0 µg/kg; Bachem, $n = 9$) 90 min prior to perfusion. Tissue was then collected and processed for immunohistochemistry (IHC) as described above. Animals were anesthetized and transcardially perfused with 0.9% saline, followed by 4% paraformaldehyde (PFA) in 0.1 M borate buffer (pH 9.5). Brains were extracted and post-fixed in 12% sucrose in PFA at 4 °C for 24 h. Following fixation, brains were rapidly frozen using dry ice-cooled isopentane and sectioned at 30 µm using a sliding microtome. Tissue sections were stored at −20 °C in antifreeze solution until immunohistochemical (IHC) processing. For IHC, all antibody incubations were conducted at 4 °C, while washes and other procedural steps were performed at room temperature. Sections were permeabilized with 0.3% Triton X-100 (Sigma, Cat #: X100-500ML) for 30 min, then blocked for 10 min with 2% normal donkey serum (Jackson ImmunoResearch, Cat #: 017-000-121). Primary antibodies were diluted in KPBS containing 2% normal donkey serum and applied overnight (~ 18 h). Following primary incubation, sections were washed in KPBS (6 changes, 10 min each). Secondary antibodies conjugated to fluorophores were also diluted in KPBS with 2% donkey serum and applied overnight. After secondary incubation, sections were again washed in KPBS (2 changes, 2 min each), then mounted on glass slides, air-dried, and coverslipped using 50% glycerol in KPBS as the mounting medium. Detection of c-Fos was performed using a rabbit anti-c-Fos primary antibody (1:500, Cell Signaling, Catalog No. 2250S), followed by a donkey anti-rabbit IgG-AlexaFluor AF488 secondary antibody (1:500, Jackson Immunoresearch, RRID: AB_2340619). Representative images and quantification of c-Fos protein expression in CA3d and DG regions were obtained from both saline- and CCK-injected animals, with analysis confined to Swanson Atlas levels 28–30. 3–4 sections per animal were quantified to yield per animal counts of c-Fos expression. Fluorescent images were captured using a Nikon 80i microscope equipped with a DS-Qi1 camera (1280 × 1024 resolution, 1.45 megapixels) under epifluorescent illumination. Image acquisition was performed using Nikon Elements BR software.

Western blotting

Dorsal HPC tissue punches from the SDV experiment were analyzed for levels of markers of cholinergic tone (choline acetyltransferase [ChAT], vesicular acetylcholine transporter [VAChT], and acetylcholinesterase [AChE]). Proteins in brain lysates (25 µg per sample/well; determined via the reducing agent and detergent compatible [RC DC™] protein assay, Bio-Rad Laboratories, Inc.) were separated using sodium dodecyl sulfate polyacrylamide gel electrophoresis, transferred onto polyvinylidene difluoride membranes, and subjected to enhanced chemiluminescence for immunodetection analysis (Chemidoc XRS, BioRad). A rabbit polyclonal anti-choline acetyltransferase antibody (1:100; Sigma-Aldrich, catalog # AB143) was used to determine the concentration of ChAT relative to a load control signal detected by a rabbit anti-β-tubulin antibody (1:1000; Cell Signaling Technology, 9F3 rabbit mAb, catalog # 2128). A rabbit polyclonal anti-vesicular ACh antibody (1:1000; Sigma-Aldrich, catalog # ABN100) was used to determine the concentration of VAChT relative to a load control signal detected by a rabbit anti-β-actin antibody (1:1000; Abcam, catalog # ab8227). A rabbit recombinant anti-acetylcholinesterase antibody (1:1000; Abcam, catalog # ab183591) was used to determine the concentration of AChE relative to a loading control signal detected by a rabbit anti-β-actin antibody (1:1000; Santa Cruz Biotechnology, catalog # NB600-503). Goat anti-rabbit-IgG-horseradish peroxidase (HRP)-linked antibody (1:5000; Cell Signaling Technology, catalog # 7074) was used as the secondary antibody. Blots were quantified with densitometry analysis using ImageJ as previously reported[10,23].

Meal location memory procedure

Meal location memory was assessed using an elevated circular Barnes maze (Diameter: 122 cm, Height: 140 cm) with 18 evenly spaced holes around its circumference. A hidden black escape box (38.73 × 11.43 × 7.62 cm) was placed beneath one of the holes. To provide visuospatial cues, four distinct markers (black and white stripes, a white circle, a red triangle, a stuffed unicorn, and a collection of irregular shapes) were positioned on the surrounding walls. One day after habituation, spatial working memory training commenced. Rats underwent mild food restriction, with food removed 1 h before the onset of their dark cycle. In the maze, they relied on visuospatial cues to locate the escape box, which contained five sucrose pellets. Each rat completed two trials per day for five consecutive training days, with a 2-min interval between trials during which the maze was cleaned and rotated. The escape box remained in the same location for both trials on a given training day, but was repositioned at the start of the first trial each subsequent day.

Errors were recorded as investigations of holes without the escape box or the two holes adjacent to the escape box, while meal location working memory was quantified as the difference in errors between trial 2 and trial 1 on each training day. These values were then averaged across the five training days. A memory probe test was conducted in which animals underwent testing identical to training, but without an escape box. Performance (memory index) in the probe test was quantified as the number of correct investigations divided by the total number of investigations performed during the second trial.

Photometry recording sessions occurred during the memory probe trial of the food location working memory task (when no food is present) and lasted 3 min (1 min acclimation and 2 min probe trial). The corrected fluorescence signal was then normalized within each rat by calculating the $\Delta F/F$ using the average fluorescence signal for the entire recording. The data was paired with real-time localization of the animal obtained from the AnyMaze Behavior Tracking Software (Stoelting, Wood Dale, IL) using an original MATLAB code and each investigation, at least 5 s apart, was isolated for analysis. In analyzing ACh signal and animal speed coupling, to minimize the influence of shared slow fluctuations and autocorrelation, analyses were performed on the first-order temporal derivatives of animal speed (meters/second) and ACh signal. For each animal, changes in speed (Speed) and concurrent changes in ACh z-score (ACh) were computed across successive time points, yielding a within-animal measure of dynamic coupling for subsequent analyses.

CCK-8 and Amylin treatment with fiber photometry

Two days before test day, animals were habituated to an intraperitoneal (IP) injection (saline) while being connected to the fiber photometry patch cord (without recording). On test day, animals underwent an overnight fast with *ad libitum* access to water, and then they were placed in a neutral cage for 15 min without intervention, after which they received IP injections of either CCK-8 (3 µg/kg;

Bachem), Amylin (50 µg/kg; Calbiochem), or their corresponding vehicle (sterile saline). To assess the effects of IP administration of these treatments on HPCd ACh release, we performed fiber photometry and recorded from the 15-min baseline period to 40 min after IP administration.

Statistical analyses

Statistical analyses were performed using GraphPad Prism 9.0 software (GraphPad Software Inc., San Diego, CA, USA) and Microsoft Excel V16.66.1. Data are expressed as mean ± SEM. Statistical details can be found in the figure legends and *n*'s refer to the number of animals for each condition. Differences were considered statistically significant at $P < 0.05$. A two-tailed paired Student's *t*-test was used to compare within-subject HPCd ACh release for active eating and inter bout periods, as well as pre-meal and post-meal periods during the standard consumption of standard chow, 11% sucrose, 4.5% corn oil, 0.2% saccharin, and 0.2% saccharin + 2% sucrose. Paired Student's *t*-test was also used to compare between-subject probe test data for the meal location working memory task.

A two-tailed unpaired Student's *t*-test was used to compare the consumption of 11% sucrose to 4.5% corn oil, and 0.2% saccharin + 2% sucrose, as well as 0.2% saccharin + 2% sucrose to 4.5% corn oil, and 2% saccharin between groups. Two-tailed unpaired Student's *t*-test was also used to compare standard laboratory chow consumption during fiber photometry meal consumption recordings between CTL SAP and 192IgG SAP, Sham and SDV (Western blot, meal location recognition), as well as CTL and CAF group (meal location recognition and meal patterns). Outliers were identified using the Grubbs' test for outliers post-hoc at a significance level of alpha = 0.05. For all experiments, assumptions of normality, homogeneity of variance (HOV), and independence were met where required.

All comparisons of the effects of either 192IgG SAP, SDV, and CAF, c-fos expression, body weight, and HPCd ACh release responses were analyzed using a two-way ANOVA with Bonferroni's post hoc test for multiple comparisons. For all statistical tests, the α level for significance was 0.05.

Reporting summary

Further information on research design is available in the Nature Portfolio Reporting Summary linked to this article.

Data availability

All data generated and analyzed for this manuscript are available in the manuscript's GitHub repository (https://github.com/ltiernol/Kanoski-Lab-Vagus-HPCd-ACh-manuscript-code). The data used to generate the visualizations of this manuscript are provided in the Source Data file. Source Data are also available through the manuscript's Open Science Framework Project (https://osf.io/y7hup/overview?view_only=237268d31b91424fa3f4b59496d4609e). Source data are provided with this paper.

Code availability

All code used to perform primary and secondary analyses in MATLAB is available in the manuscript's GitHub repository (https://github.com/ltiernol/Kanoski-Lab-Vagus-HPCd-ACh-manuscript-code), as well as within the manuscript's Open Science Framework Project (https://osf.io/y7hup/overview?view_only=237268d31b91424fa3f4b59496d4609e).

References

1. Moran, T. H., Baldessarini, A. R., Salorio, C. F., Lowery, T. & Schwartz, G. J. Vagal afferent and efferent contributions to the inhibition of food intake by cholecystokinin. *Am. J. Physiol. Regulat. Integr. Comp. Physiol.* **272**, R1245–R1251 (1997).
2. Little, T. J. et al. Mapping glucose-mediated gut-to-brain signalling pathways in humans. *Neuroimage* **96**, 1–11 (2014).
3. Woodward, O. R. M., Gribble, F. M., Reimann, F. & Lewis, J. E. Gut peptide regulation of food intake—evidence for the modulation of hedonic feeding. *J. Physiol.* **600**, 1053–1078 (2022).
4. Grill, H. J. & Hayes, M. R. Hindbrain neurons as an essential hub in the neuroanatomically distributed control of energy balance. *Cell Metab.* **16**, 296–309 (2012).
5. Décarie-Spain, L., Hayes, A. M. R., Lauer, L. T. & Kanoski, S. E. The gut-brain axis and cognitive control: a role for the vagus nerve. *Semin. Cell Dev. Biol.* **156**, 201–209 (2024).
6. Hameed, M. et al. Gut-brain axis: investigating the effects of gut health on cognitive functioning in adults. *Cureus* **16**, e64286 (2024).
7. Prescott, S. L. & Liberles, S. D. Internal senses of the vagus nerve. *Neuron* **110**, 579–599 (2022).
8. Olsen, L. K., Solis, E. Jr., McIntire, L. K. & Hatcher-Solis, C. N. Vagus nerve stimulation: mechanisms and factors involved in memory enhancement. *Front Hum. Neurosci.* **17**, 1152064 (2023).
9. Bari, B. A., Chokshi, V. & Schmidt, K. Locus coeruleus-norepinephrine: basic functions and insights into Parkinson's disease. *Neural Regen. Res.* **15**, 1006–1013 (2020).
10. Suarez, A. N. et al. Gut vagal sensory signaling regulates hippocampus function through multi-order pathways. *Nat. Commun.* **9**, 2181 (2018).
11. Onimus, O. et al. The gut-brain vagal axis scales hippocampal memory processes and plasticity. *Neurobiol. Dis.* **199**, 106569 (2024).
12. Yang, M. et al. Separate orexigenic hippocampal ensembles shape dietary choice by enhancing contextual memory and motivation. *Nat. Metab.* **7**, 276–296 (2025).
13. Bird, C. M. & Burgess, N. The hippocampus and memory: insights from spatial processing. *Nat. Rev. Neurosci.* **9**, 182–194 (2008).
14. Henke, K., Weber, B., Kneifel, S., Wieser, H. G. & Buck, A. Human hippocampus associates information in memory. *Proc. Natl. Acad. Sci. USA* **96**, 5884–5889 (1999).
15. Jarrard, L. E. On the role of the hippocampus in learning and memory in the rat. *Behav. Neural Biol.* **60**, 9–26 (1993).
16. Haam, J. & Yakel, J. L. Cholinergic modulation of the hippocampal region and memory function. *J. Neurochem.* **142**, 111–121 (2017).
17. Maurer, S. V. & Williams, C. L. The cholinergic system modulates memory and hippocampal plasticity via its interactions with non-neuronal cells. *Front. Immunol.* **8**, 2017 (2017).
18. Palacios-Filardo, J. et al. Acetylcholine prioritises direct synaptic inputs from entorhinal cortex to CA1 by differential modulation of feedforward inhibitory circuits. *Nat. Commun.* **12**, 5475 (2021).
19. Boitard, C. et al. Impairment of hippocampal-dependent memory induced by juvenile high-fat diet intake is associated with enhanced hippocampal inflammation in rats. *Brain Behav. Immun.* **40**, 9–17 (2014).
20. Tsan, L. et al. Early life Western diet-induced memory impairments and gut microbiome changes in female rats are long-lasting despite healthy dietary intervention. *Nutr. Neurosci.* **25**, 2490–2506 (2022).
21. Hsu, T. M. et al. Effects of sucrose and high fructose corn syrup consumption on spatial memory function and hippocampal neuroinflammation in adolescent rats. *Hippocampus* **25**, 227–239 (2015).
22. Khazen, T., Hatoum, O. A., Ferreira, G. & Maroun, M. Acute exposure to a high-fat diet in juvenile male rats disrupts hippocampal-dependent memory and plasticity through glucocorticoids. *Sci. Rep.* **9**, 12270 (2019).
23. Hayes, A. M. R. et al. Western diet consumption impairs memory function via dysregulated hippocampus acetylcholine signaling. *Brain Behav. Immun.* **118**, 408–422 (2024).
24. Covasa, M., Grahn, J. & Ritter, R. C. High fat maintenance diet attenuates hindbrain neuronal response to CCK. *Regul. Pept.* **86**, 83–88 (2000).

25. Savastano, D. M. & Covasa, M. Adaptation to a high-fat diet leads to hyperphagia and diminished sensitivity to cholecystokinin in rats. *J. Nutr.* **135**, 1953–1959 (2005).
26. Daly, D. M., Park, S. J., Valinsky, W. C. & Beyak, M. J. Impaired intestinal afferent nerve satiety signalling and vagal afferent excitability in diet induced obesity in the mouse. *J. Physiol.* **589**, 2857–2870 (2011).
27. Kentish, S. et al. Diet-induced adaptation of vagal afferent function. *J. Physiol.* **590**, 209–221 (2012).
28. de Lartigue, G. Role of the vagus nerve in the development and treatment of diet-induced obesity. *J. Physiol.* **594**, 5791–5815 (2016).
29. Min, D. K., Tuor, U. I. & Chelikani, P. K. Gastric distention induced functional magnetic resonance signal changes in the rodent brain. *Neuroscience* **179**, 151–158 (2011).
30. Min, D. K., Tuor, U. I., Koopmans, H. S. & Chelikani, P. K. Changes in differential functional magnetic resonance signals in the rodent brain elicited by mixed-nutrient or protein-enriched meals. *Gastroenterology* **141**, 1832–1841 (2011).
31. Chandra, R. & Liddle, R. A. Cholecystokinin. *Curr. Opin. Endocrinol., Diab. Obes.* **14**, 63–67 (2007).
32. Lutz, T. A., Mollet, A., Rushing, P. A., Riediger, T. & Scharrer, E. The anorectic effect of a chronic peripheral infusion of amylin is abolished in area postrema/nucleus of the solitary tract (AP/NTS) lesioned rats. *Int. J. Obes.* **25**, 1005–1011 (2001).
33. Williams, E. K. et al. Sensory neurons that detect stretch and nutrients in the digestive system. *Cell* **166**, 209–221 (2016).
34. Goldstein, N. et al. Hypothalamic detection of macronutrients via multiple gut-brain pathways. *Cell Metab.* **33**, 676–687.e675 (2021).
35. Levin, B. E. & Dunn-Meynell, A. A. Defense of body weight depends on dietary composition and palatability in rats with diet-induced obesity. *Am. J. Physiol. Regul. Integr. Comp. Physiol.* **282**, R46–R54 (2002).
36. Kanoski, S. E., Zhang, Y., Zheng, W. & Davidson, T. L. The effects of a high-energy diet on hippocampal function and blood-brain barrier integrity in the rat. *J. Alzheimers Dis.* **21**, 207–219 (2010).
37. Loper, H. et al. Both high fat and high carbohydrate diets impair vagus nerve signaling of satiety. *Sci. Rep.* **11**, 10394 (2021).
38. Noble, E. E. et al. Gut microbial taxa elevated by dietary sugar disrupt memory function. *Transl. Psychiatry* **11**, 194 (2021).
39. Hayes, A. M. R. et al. Early- but not late-adolescent Western diet consumption programs for long-lasting memory impairments in male but not female rats. *Appetite* **194**, 107150 (2024).
40. Anzalone, S., Vetreno, R. P., Ramos, R. L. & Savage, L. M. Cortical cholinergic abnormalities contribute to the amnesic state induced by pyrithiamine-induced thiamine deficiency in the rat. *Eur. J. Neurosci.* **32**, 847–858 (2010).
41. Zhang, Y. et al. Cholinergic suppression of hippocampal sharp-wave ripples impairs working memory. *Proc. Natl. Acad. Sci.* **118**, e2016432118 (2021).
42. Vertes, R. P. & Kocsis, B. Brainstem-diencephalo-septohippocampal systems controlling the theta rhythm of the hippocampus. *Neuroscience* **81**, 893–926 (1997).
43. Dannenberg, H. et al. Synergy of direct and indirect cholinergic septo-hippocampal pathways coordinates firing in hippocampal networks. *J. Neurosci.* **35**, 8394–8410 (2015).
44. Hasselmo, M. E. The role of acetylcholine in learning and memory. *Curr. Opin. Neurobiol.* **16**, 710–715 (2006).
45. Ballinger, E. C., Ananth, M., Talmage, D. A. & Role, L. W. Basal forebrain cholinergic circuits and signaling in cognition and cognitive decline. *Neuron* **91**, 1199–1218 (2016).
46. Berthoud, H. R. Homeostatic and non-homeostatic pathways involved in the control of food intake and energy balance. *Obes. (Silver Spring)* **14**, 197s–200s (2006).
47. Raybould, H. E. Gut chemosensing: interactions between gut endocrine cells and visceral afferents. *Auton. Neurosci.* **153**, 41–46 (2010).
48. Kaelberer, M. M. et al. A gut-brain neural circuit for nutrient sensory transduction. *Science* **361**, eaat5236 (2018).
49. Rogers, R. C. & Hermann, G. E. Mechanisms of action of CCK to activate central vagal afferent terminals. *Peptides* **29**, 1716–1725 (2008).
50. Winzenried, E. T., Neyens, D. M., Calkins, R. & Appleyard, S. M. CCK-expressing neurons in the NTS are directly activated by CCK-sensitive C-type vagal afferents. *Am. J. Physiol. Regul. Integr. Comp. Physiol.* **328**, R121–r132 (2025).
51. Arinel, M. et al. Gut distension evokes rapid neural dynamics in vagal and hindbrain populations of larval zebrafish. https://doi.org/10.1101/2025.07.21.665834 (2025).
52. Królczyk, G., Zurowski, D., Sobocki, J., Laskiewicz, J. & Thor, P. J. Encoding meal in integrated vagal afferent discharge. *J. Physiol. Pharm.* **55**, 99–106 (2004).
53. Wachsmuth, H. R., Weninger, S. N. & Duca, F. A. Role of the gut–brain axis in energy and glucose metabolism. *Exp. Mol. Med.* **54**, 377–392 (2022).
54. Krieger, J. P. et al. Knockdown of GLP-1 receptors in vagal afferents affects normal food intake and glycemia. *Diabetes* **65**, 34–43 (2016).
55. Dailey, M. J. & Moran, T. H. Glucagon-like peptide 1 and appetite. *Trends Endocrinol. Metab.* **24**, 85–91 (2013).
56. Sen, T. et al. Diet-driven microbiota dysbiosis is associated with vagal remodeling and obesity. *Physiol. Behav.* **173**, 305–317 (2017).
57. Jiang, Y. Y., Li, L., Shen, W. X., Qiu, Y. H. & Peng, Y. P. Acetylcholine suppresses microglial inflammatory response in rats via acting on microglial α7nAChR. *Sheng Li Xue Bao.* **70**, 33–39 (2018).
58. Patel, H., McIntire, J., Ryan, S., Dunah, A. & Loring, R. Anti-inflammatory effects of astroglial α7 nicotinic acetylcholine receptors are mediated by inhibition of the NF-κB pathway and activation of the Nrf2 pathway. *J. Neuroinflammation* **14**, 192 (2017).
59. Li, L. et al. Acetylcholine suppresses microglial inflammatory response via α7nAChR to protect hippocampal neurons. *J. Integr. Neurosci.* **18**, 51–56 (2019).
60. Hasselmo, M. E., Schnell, E. & Barkai, E. Dynamics of learning and recall at excitatory recurrent synapses and cholinergic modulation in rat hippocampal region CA3. *J. Neurosci.* **15**, 5249–5262 (1995).
61. Hasselmo, M. E. & McGaughy, J. High acetylcholine levels set circuit dynamics for attention and encoding and low acetylcholine levels set dynamics for consolidation. *Prog. Brain Res.* **145**, 207–231 (2004).
62. Giovannini, M. G. et al. Effects of novelty and habituation on acetylcholine, GABA, and glutamate release from the frontal cortex and hippocampus of freely moving rats. *Neuroscience* **106**, 43–53 (2001).
63. Baxter, M. G., Bucci, D. J., Gorman, L. K., Wiley, R. G. & Gallagher, M. Selective immunotoxic lesions of basal forebrain cholinergic cells: effects on learning and memory in rats. *Behav. Neurosci.* **109**, 714–722 (1995).
64. Yu, A. J. & Dayan, P. Uncertainty, neuromodulation, and attention. *Neuron* **46**, 681–692 (2005).
65. Easton, A., Douchamps, V., Eacott, M. & Lever, C. A specific role for septohippocampal acetylcholine in memory? *Neuropsychologia* **50**, 3156–3168 (2012).
66. Décarie-Spain, L. et al. Ventral hippocampus-lateral septum circuitry promotes foraging-related memory. *Cell Rep.* **40**, 111402 (2022).
67. Fanselow, M. S. & Dong, H. W. Are the dorsal and ventral hippocampus functionally distinct structures? *Neuron* **65**, 7–19 (2010).

68. Strange, B. A., Witter, M. P., Lein, E. S. & Moser, E. I. Functional organization of the hippocampal longitudinal axis. *Nat. Rev. Neurosci.* **15**, 655–669 (2014).
69. Moser, M. B. & Moser, E. I. Functional differentiation in the hippocampus. *Hippocampus* **8**, 608–619 (1998).
70. Gilbert, P. E., Kesner, R. P. & Lee, I. Dissociating hippocampal subregions: double dissociation between dentate gyrus and CA1. *Hippocampus* **11**, 626–636 (2001).
71. Komorowski, R. W. et al. Ventral hippocampal neurons are shaped by experience to represent behaviorally relevant contexts. *J. Neurosci.* **33**, 8079–8087 (2013).
72. Ciocchi, S., Passecker, J., Malagon-Vina, H., Mikus, N. & Klausberger, T. Brain computation. Selective information routing by ventral hippocampal CA1 projection neurons. *Science* **348**, 560–563 (2015).
73. Chen, Z. R., Huang, J. B., Yang, S. L. & Hong, F. F. Role of cholinergic signaling in Alzheimer's disease. *Molecules* **27**, https://doi.org/10.3390/molecules27061816 (2022).
74. Więckowska-Gacek, A., Mietelska-Porowska, A., Wydrych, M. & Wojda, U. Western diet as a trigger of Alzheimer's disease: From metabolic syndrome and systemic inflammation to neuroinflammation and neurodegeneration. *Ageing Res. Rev.* **70**, 101397 (2021).
75. Kanoski, S. E., Zhang, Y., Zheng, W. & Davidson, T. L. The effects of a high-energy diet on hippocampal function and blood-brain barrier integrity in the rat. *J. Alzheimer's. Dis.* **21**, 207–219 (2010).
76. Graham, L. C. et al. Chronic consumption of a western diet induces robust glial activation in aging mice and in a mouse model of Alzheimer's disease. *Sci. Rep.* **6**, 21568 (2016).
77. Lin, S.-Y. et al. Dementia and vagotomy in Taiwan: a population-based cohort study. *BMJ Open* **8**, e019582 (2018).
78. Yuan, H. & Silberstein, S. D. Vagus nerve and vagus nerve stimulation, a comprehensive review: part II. *Headache* **56**, 259–266 (2016).
79. Yu, Y. et al. Transauricular vagal nerve stimulation at 40 Hz inhibits hippocampal P2X7R/NLRP3/caspase-1 signaling and improves spatial learning and memory in 6-month-old APP/PS1 mice. *Neuromodulation* **26**, 589–600 (2023).
80. Borden, P. M. et al. A fast genetically encoded fluorescent sensor for faithful *in vivo* acetylcholine detection in mice, fish, worms and flies. *bioRxiv* https://doi.org/10.1101/2020.02.07.939504 (2020).
81. Lin, L., Gupta, S., Zheng, W. S., Si, K. & Zhu, J. J. Genetically encoded sensors enable microt- and nano-scopic decoding of transmission in healthy and diseased brains. *Mol. Psychiatry* **26**, 443–455 (2021).
82. Zhang, K., Han, Y., Zhang, P., Zheng, Y. & Cheng, A. Comparison of fluorescence biosensors and whole-cell patch clamp recording in detecting ACh, NE, and 5-HT. *Front. Cell Neurosci.* **17**, 1166480 (2023).
83. Chen, J. et al. The property-based practical applications and solutions of genetically encoded acetylcholine and monoamine sensors. *J. Neurosci.* **41**, 2318–2328 (2021).
84. Moran, T. H., Norgren, R., Crosby, R. J. & McHugh, P. R. Central and peripheral vagal transport of cholecystokinin binding sites occurs in afferent fibers. *Brain Res.* **526**, 95–102 (1990).
85. Peters, J. H., Simasko, S. M. & Ritter, R. C. Modulation of vagal afferent excitation and reduction of food intake by leptin and cholecystokinin. *Physiol. Behav.* **89**, 477–485 (2006).

Acknowledgements

This work was supported by the National Institute of Diabetes and Digestive and Kidney Diseases (Grant Nos. DK104897 and DK123423 [to S.E.K.]; F31AG092136 [to L.T.L.]; by a Postdoctoral Ruth L. Kirschstein National Research Service Award from the National Institute on Aging (Grant No. F32AG077932 [to A.M.R.H.]), a Quebec Research Funds postdoctoral fellowship (Fellowship No. 315201 [to L.D.-S.]), and an Alzheimer's Association Research Fellowship to Promote Diversity (Fellowship No. AARFD-22-972811 [to L.D.-S.]). We thank the Kanoski Lab undergraduate research assistants for their support with the behavioral experiments, as well as all funding sources. The authors report no biomedical financial interests or potential conflicts of interest.

Author contributions

L.T.L., L.D.S. and S.E.K. conceived and performed the experiments and wrote the manuscript. A.M.R.H., A.N.S., A.B., M.E.K., A.E.K., R.C., J.J.R., K.S.S., A.N., K.N.D. performed experiments. L.A.S. and K.M. provided expertise on experimental design.

Funding

L.T.L. discloses support for the research of this work from the National Institute of Aging (NIA) [F31AG092136]. S.E.K discloses support for the research of this work from the National Institute of Diabetes and Digestive and Kidney Diseases (NIDDK) [DK104897 and DK123423]. A.M.R.H. discloses support for publication of this work from the NIA National Research Service Award [F32AG077932]. L.D.S. discloses support for the research of this work from the Quebec Research Funds [315201], and the Alzheimer's Association Research Fellowship to Promote Diversity [AARFD-22-972811].

Competing interests

S.E.K. receives research funding from Novo Nordisk that was not used in support of these studies. All other authors declare no competing interests.

Additional information

Supplementary information The online version contains supplementary material available at https://doi.org/10.1038/s41467-026-73896-2.

Correspondence and requests for materials should be addressed to Léa. Décarie-Spain or Scott E. Kanoski.

Peer review information *Nature Communications* thanks Guillaume Ferreira and the other anonymous reviewer(s) for their contribution to the peer review of this work. A peer review file is available.